HEATSTORE
Benchmarking, and improving models of subsurface heat storage dynamics

Comparison of Danish PTES and BTES installation measurements with their corresponding TRNSYS models

Prepared by: Geoffroy Gauthier, PlanEnergi

Checked by: Jan Erik Nielsen, PlanEnergi
Niels From, PlanEnergi

Approved by: Thomas Vangkilde-Pedersen, GEUS

Please cite this report as: Gauthier, G. (2020): Benchmarking, and improving models of subsurface heat storage dynamics. Comparison of Danish PTES and BTES installation measurements with their corresponding TRNSYS models. GEOTHERMICA – ERA NET Cofund Geothermal. 47 pp.

This report represents a Danish contribution to the work in Task 2.3 in the HEATSTORE project

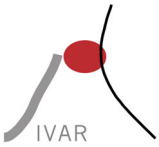

HEATSTORE (170153-4401) is one of nine projects under the GEOTHERMICA – ERA NET Cofund aimed at accelerating the uptake of geothermal energy by 1) advancing and integrating different types of underground thermal energy storage (UTES) in the energy system, 2) providing a means to maximise geothermal heat production and optimise the business case of geothermal heat production doublets, 3) addressing technical, economic, environmental, regulatory and policy aspects that are necessary to support efficient and cost-effective deployment of UTES technologies in Europe.

This project has been subsidized through the ERANET cofund GEOTHERMICA (Project n. 731117), from the European Commission, RVO (the Netherlands), DETEC (Switzerland), FZJ-PtJ (Germany), ADEME (France), EUDP (Denmark), Rannis (Iceland), VEA (Belgium), FRCT (Portugal), and MINECO (Spain).

About HEATSTORE

High Temperature Underground Thermal Energy Storage

The heating and cooling sector is vitally important for the transition to a low-carbon and sustainable energy system. Heating and cooling is responsible for half of all consumed final energy in Europe. The vast majority – 85% - of the demand is fulfilled by fossil fuels, most notably natural gas. Low carbon heat sources (e.g. geothermal, biomass, solar and waste-heat) need to be deployed and heat storage plays a pivotal role in this development. Storage provides the flexibility to manage the variations in supply and demand of heat at different scales, but especially the seasonal dips and peaks in heat demand. Underground Thermal Energy Storage (UTES) technologies need to be further developed and need to become an integral component in the future energy system infrastructure to meet variations in both the availability and demand of energy.

The main objectives of the HEATSTORE project are to lower the cost, reduce risks, improve the performance of high temperature (~25°C to ~90°C) underground thermal energy storage (HT-UTES) technologies and to optimize heat network demand side management (DSM). This is primarily achieved by 6 new demonstration pilots and 8 case studies of existing systems with distinct configurations of heat sources, heat storage and heat utilization. This will advance the commercial viability of HT-UTES technologies and, through an optimized balance between supply, transport, storage and demand, enable that geothermal energy production can reach its maximum deployment potential in the European energy transition.

Furthermore, HEATSTORE also learns from existing UTES facilities and geothermal pilot sites from which the design, operating and monitoring information will be made available to the project by consortium partners.

HEATSTORE is one of nine projects under the GEOTHERMICA – ERA NET Cofund and has the objective of accelerating the uptake of geothermal energy by 1) advancing and integrating different types of underground thermal energy storage (UTES) in the energy system, 2) providing a means to maximize geothermal heat production and optimize the business case of geothermal heat production doublets, 3) addressing technical, economic, environmental, regulatory and policy aspects that are necessary to support efficient and cost-effective deployment of UTES technologies in Europe. The three-year project will stimulate a fast-track market uptake in Europe, promoting development from demonstration phase to commercial deployment within 2 to 5 years, and provide an outlook for utilization potential towards 2030 and 2050.

The 23 contributing partners from 9 countries in HEATSTORE have complementary expertise and roles. The consortium is composed of a mix of scientific research institutes and private companies. The industrial participation is considered a very strong and relevant advantage which is instrumental for success. The combination of leading European research institutes together with small, medium and large industrial enterprises, will ensure that the tested technologies can be brought to market and valorised by the relevant stakeholders.

Document Change Record

This section shows the historical versions, with a short description of the updates.

Version	Short description of change
2020.11.02	Ver. 0 Final report

Table of Content

1 Introduction

The testing concept presented here concentrates on a main problem set that is meant to express important capabilities available in Thermo-Hydro (TH) simulators. In the context of verification, results from a given simulator should be compared to results from known analytical, empirical, and analytical-empirical solutions, as well as results produced by other simulators. At least within TH modelling, this should ultimately establish a point of reference across all tested simulators in terms of capabilities and accuracy.

In the Danish case, the simulation tools do not enable to have the same standard tests as the other simulators (e.g. FEFLOW). It is nevertheless possible to compare experimental and modelling results from a thermal energy balance point of view. This has been done in the following examples for two different types of TES. For both, the heat transfer calculation program TRNSYS was used to carry out the comparisons.

2 Pit Thermal Energy Storage (PTES)

2.1 Danish case study in Dronninglund

This Danish case study is that of a Pit Thermal Energy Storage (PTES), set up as a part of the EUDP project *SUNSTORE 3*[1], in a system that combines 37'573 m^2 of solar collectors, a 60'000 m^3 PTES and a 2.1 MW (cooling capacity) absorption heat pump. The system supplies heat to a district heating network located in Dronninglund, Denmark.

2.1.1 Conceptualization

2.1.1.1 UTES concept and specifications, scope and aims of the study

The PTES in Dronninglund is located next to the solar collector field and connected to the local District Heating Network (DHN). The absorption heat pump is located at the junction between the city's DHN and the pipes delivering the solar heat (Figure 2.1).

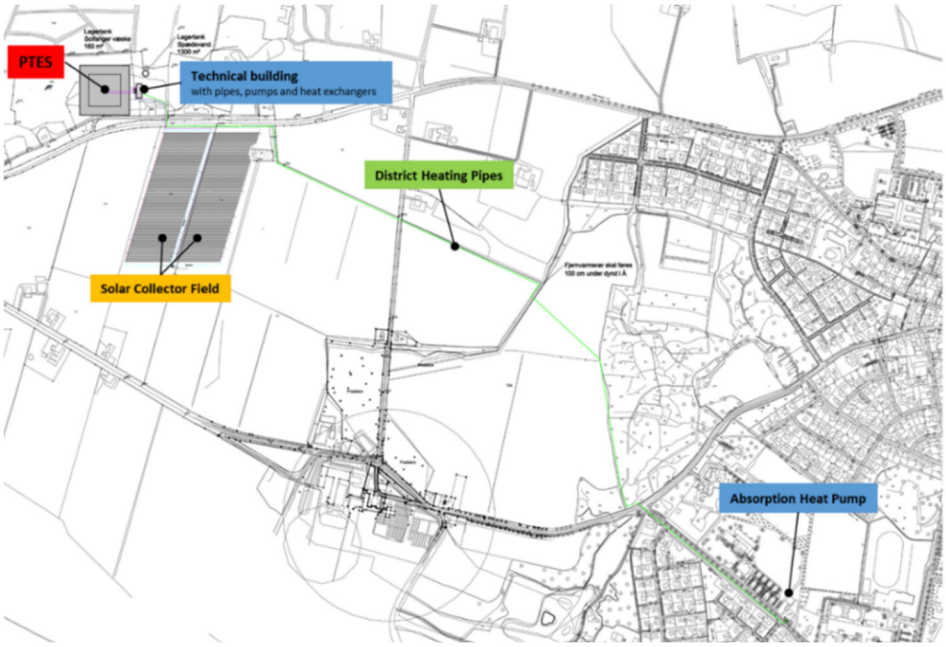

Figure 2.1. Dronninglund solar thermal production plant with seasonal thermal energy storage.

The PTES was built between 2013 and 2014, and the main characteristics are reproduced in Table 2.1. Pictures of the PTES while being built and after being implemented are shown in Figure 2.2. The lid refers to the top insulation of the PTES.

[1] *SUNSTORE 3 - Phase 2 - Implementation*, 2015, EUDP project numbers 64009-0043 and 64010-0447.

Table 2.1. Main geometry characteristics of the PTES in Dronninglund.

Parameter	Value	Unit
Water volume	60'000	m^3
Slope of the dam	1:2	-
Edge length at bottom	26.38	m
Edge length under the lid	90.38	m
Edge length over the lid	91.38	m
Lid area	8'351	m^2
Water depth	16	m
Bottom depth under terrain	11.95	m
Dam height over terrain (average)	4.30	m
Insulation thickness	24	cm
Insulation conductivity	0.04	W / (m·K)
Number of inlets/outlets	3	-
Top diffuser height	15.75	m
Middle diffuser height[2]	11.2	m
Bottom diffuser height	0.5	m

Figure 2.2. Dronninglund PTES under construction (left) and after being built, next to the solar collector field and the technical building (right).

The PTES is built as an inverted truncated pyramid and is insulated at the top with 3 layers of 80 mm of the material *Nomalén*. Both the floating liners and the weight pipes that gather rainwater to the center of the lid are shown in Figure 2.3. The weight pipes layout on the lid is shown in Figure 2.4.

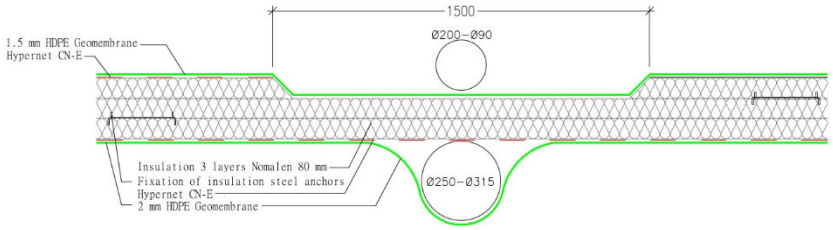

Figure 2.3. Cross section of the lid of Dronninglund's PTES, including weight pipes (top), floating liner (bottom) and the insulation layers surrounded by the geomembrane.

[2] The middle diffuser's height is set such that 50% of the water volume is under the diffuser, and 50% over the diffuser, dividing the PTES in roughly two equal heat capacities.

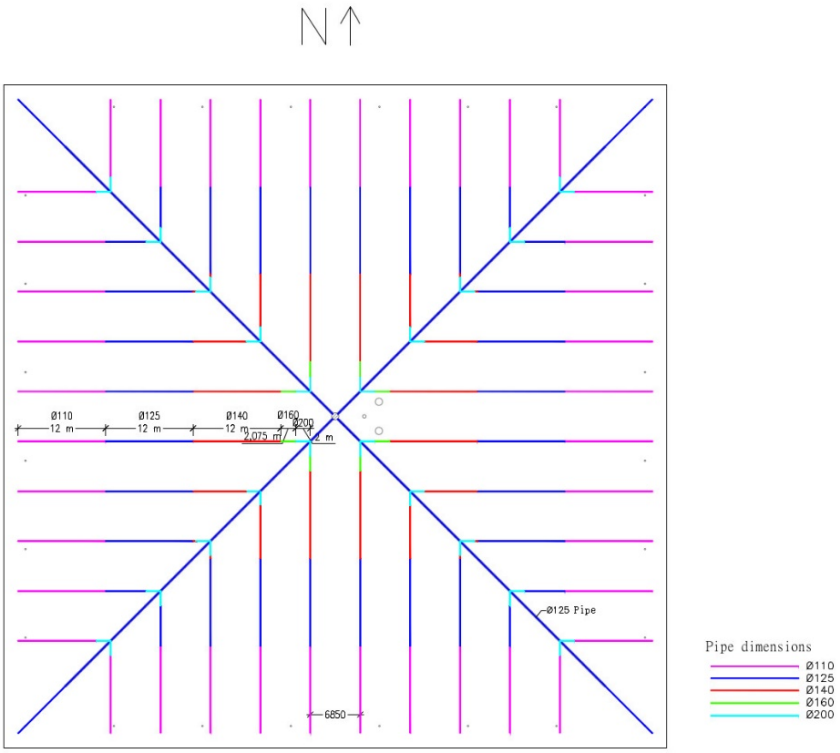

Figure 2.4. Weight pipe layout on the top of the lid of the PTES in Dronninglund, gathering the rainwater to the center of the lid, from where it is pumped away.

2.1.1.2 Dronninglund solar heating system concept presentation

The PTES in Dronninglund is used as a seasonal heat storage, storing heat in the summer, where solar heat production is high and heat demand from the DHN is low, and releasing this heat in the winter when heat demand is highest. The way this is done with a PTES, is divided into two main loops.

The first loop comprises the solar collector field and the PTES, exchanging heat through a heat exchanger, noted HX1 in Figure 2.5. In this loop, the top of the PTES is heated (up to 90°C) with heat coming from the exit of the solar collector field, and the bottom of the PTES (at a lower temperature, down to about 10°C) is used as inlet for the solar collector field. Additionally, a middle inlet/outlet was set up, in order to be able to better manage stratification of the temperatures inside of the PTES. One example is the following: if the PTES top temperature is at 90°C, but water coming out of the solar collector field is at 60°C, it would thus be better to send this heat to the middle diffusor rather than the top, in order to keep a high top PTES temperature.

The second loop comprises the PTES, the absorption heat pump, the DHN and a heat exchanger, noted HX-2. The system is run the following way: if the PTES top temperature is higher than the district heating forward temperature, then the top PTES water is sent to HX-2. Else the absorption heat pump is used. In both cases, another heat exchanger (in grey above the absorption heat pump on Figure 2.5) is used to bring the water temperature to the forward district heating temperature. These loops are represented in Figure 2.5.

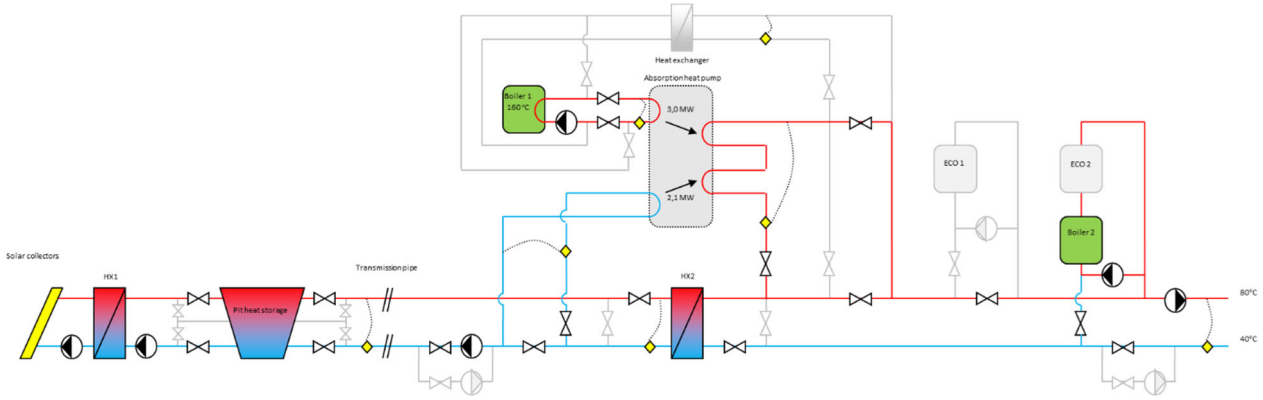

Figure 2.5. Principle diagram of the solar heating system from *SUNSTORE 3*[1]. Yellow squares are flow/energy meters. The diagram is simplified and not all equipment is shown.

2.1.1.3 Dronninglund solar heating system design and first monitoring results

The initial design was made such that the solar heating system comprised of the solar collector field, the PTES and the solar heat part of the absorption heat pump (excluding the heat provided at the generator, by the bio oil boiler noted Boiler 1 on Figure 2.5) can cover 41%[3] of the DHN's heat demand (Figure 2.6).

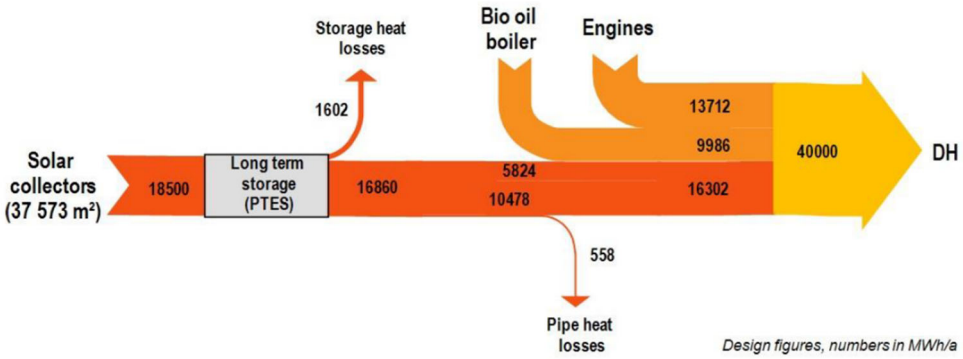

Figure 2.6. Yearly energy flow diagram according to design figures[1].

To achieve this production, the modelling program *TRNSYS* was used at the design phase of the system, and that's how the main components were sized. After being built, this project brought a first opportunity to make measurements on the implemented system and compare the obtained results with the modelling calculations for the year 2014. This enabled a first validation of system design calculations and already showed good accordance between measurements and calculations (Figure 2.7), including the PTES heat balance. The DHN load is lower than what was expected because the monitoring results were only available from March 2014, and the solar fraction was 34%. A lower solar fraction for the first years is expected because of higher initial heat loss to heat up the surrounding soil. Also, PTES cooling was necessary because of too many operating hours of the CHP in the spring of 2014.

[3] The fraction of the heat provided by the solar heating system is called *solar fraction*.

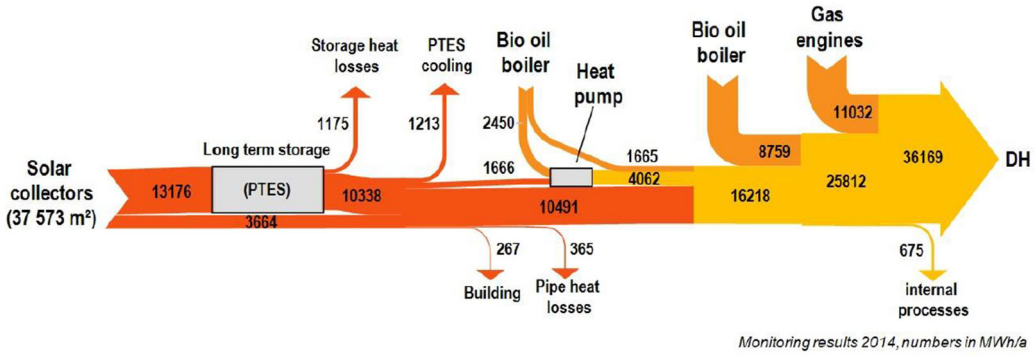

Figure 2.7. Yearly energy flow diagram according to monitoring results from 2014[1].

This first monitoring campaign also gave access to the evolution of the water temperatures inside the PTES (Figure 2.8). It shows that the top of the PTES is heated up to 86°C the first year, the maximum temperature being obtained at the end of July. The bottom temperature of the BTES drops down to a minimum value of 12°C at the end of December. The energy content of the storage is also shown and is calculated with a reference temperature of 10 °C.

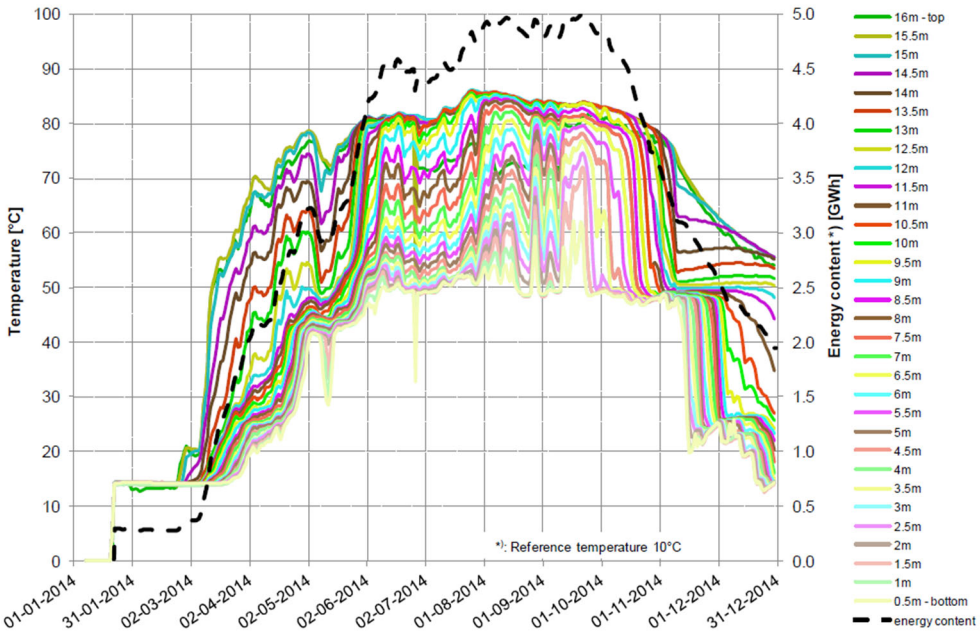

Figure 2.8. PTES measured internal temperature development in 2014[1].

2.1.1.4 Scope and aims of the PTES measurement study

These first monitoring results show clearly the limitations of such a comparison: a lot of components are present, there are losses in various points of the network, the yearly radiation and weather conditions in 2014 are necessarily different from the standard weather profile used in the model calculations for the design phase, and specifically for the PTES, the energy content at the beginning and the end of the year aren't the same (Figure 2.8), which means that the modelling cannot properly be compared to the experimental results. In order to study the PTES modelling in more details, this component is studied isolated from the rest of the energy system, and monitoring results (such as ambient air temperature) are used as inputs to the model.

Therefore, a further measurement campaign is used to calibrate specifically the PTES model in TRNSYS, to determine precisely how the PTES component behaves compared to real-life conditions.

2.1.1.5 Geometry of the PTES and geology of the environment

The PTES was partly built above ground level, as illustrated in Figure 2.9. The water depth is 16 m, the bottom of the PTES has an area of 26 x 26 m^2, while the top has an area of 90 x 90 m^2 (slope 1:2 or 26°). Table 2.1 gathers all the detailed information about PTES geometry. The main geometry parameters have been considered in the model setup (see section 2.1.3 of the current report). The actual PTES was built on a non-horizontal field. Figure 2.9 is a principle sketch representing the main PTES geometry parameters.

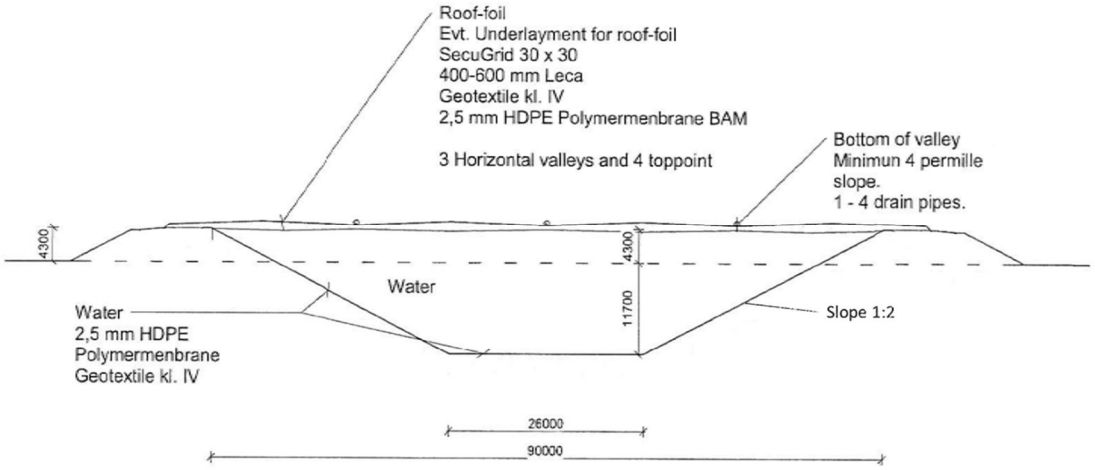

Figure 2.9. PTES main geometry parameters.

In order to calibrate properly the PTES model, a geological study from 2010[4] was used, and the following conditions were observed, from top to bottom:

- Soil depth from 0 m to 27 m: dry sandy soil with a thermal conductivity of approximately 0.3 W/m/K to 0.5 W/m/K and no groundwater flow, density 2'000 kg/m³
- Soil depth below 27 m: water-saturated sandy soil with a thermal conductivity of approximately 1.0 W/m/K (groundwater level is at a depth of 27 m), density 2'100 kg/m³

For the model simulations, a thermal conductivity of 0.4 W/m/K and a density of 2'000 kg/m^3 were chosen.

2.1.2 PTES measurements description

A series of sensors have been installed in and around the PTES, in order to follow up on the behavior of the PTES. The measurements made by these sensors can also be used as a reference for the calibration of the TRNSYS PTES models. The types and location of the sensors are described in the following section.

2.1.2.1 Sensor types and placement

The PTES has been equipped with (see Figure 2.10):

- 32 water temperature sensors, one for every 0.5 m (see measurements results Figure 2.8), except for the top sensor, placed 0.1 m under the bottom of the lid
- a water level sensor, mounted on top of the top diffuser (not used in the current study)
- a heat flux sensor in the middle of the insulation
- 2 temperature sensors around the lid insulation, one on the top, one under the bottom

Additionally, 3 temperature sensors have been placed in the pipes leading to the top, middle and bottom diffusers of the PTES (see Figure 2.2 and Table 2.1 for their position inside the PTES), and a flowmeter was placed on the pipe leading to the middle diffusor. The flowmeter measures both direction and magnitude of the flowrate. The other flowrates are deduced/calculated from the measurements of 2 other flowmeters, placed respectively between HX-1 and the PTES, and between HX-2 and the PTES (see Figure 2.5), and by assuming volume flow balance, not mass flow balance.

[4] *SUNSTORE 3 - Fase 1 - Projektering og udbud*, 2011, EUDP project number 63011-0178.

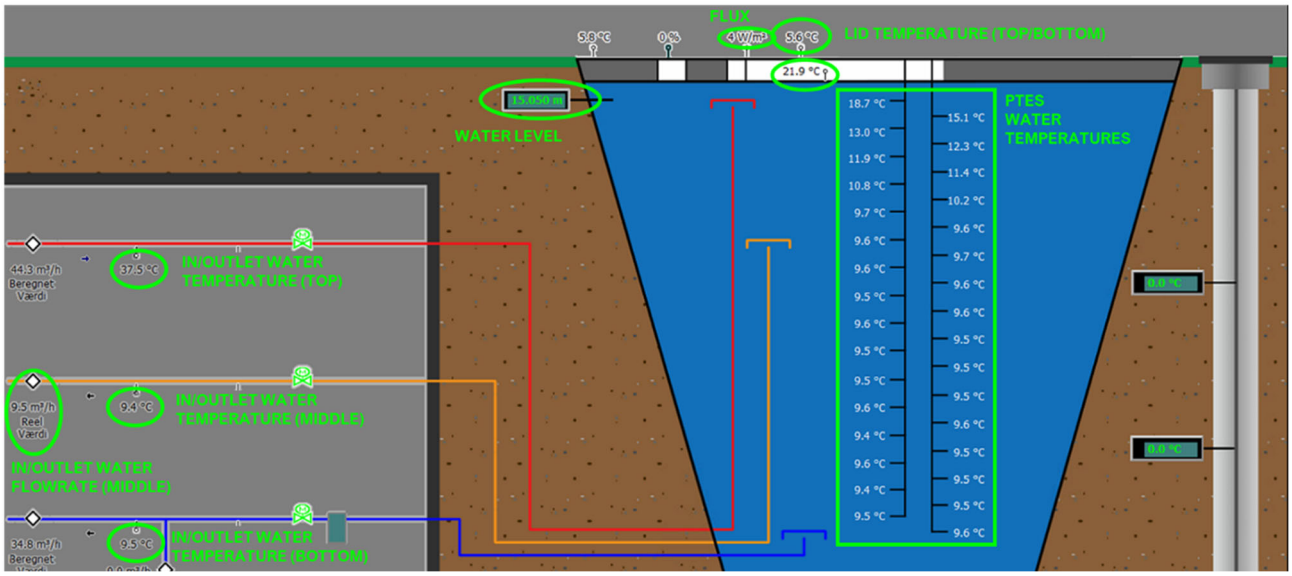

Figure 2.10. Location and function of the main sensors used for the PTES calibration (in light green).

2.1.2.2 Measurement campaign and method

Measurements started from March 2014 to follow-up performances of the PTES and the entire solar heating system. The specific equipment used to make measurements around the PTES (as described in section 2.1.2.1) provide results every 10 minutes and have been studied in detail from 2015 by SOLITES[1].

PlanEnergi has used the data from the year 2017 to make a calibration of three different PTES components in TRNSYS. The measured input temperatures and flows etc. for the Dronninglund storage are given as inputs to the PTES models, and the resulting calculated output temperatures, flows etc. from the simulation are then compared to the corresponding measured data. This way, the performance of the three different TRNSYS PTES components in emulating the operation of the Dronninglund storage can be evaluated and compared. This provides information on which model is most suitable for modelling PTES (measured on accuracy, calculation time etc.) and how large one can expect the deviation between modelled PTES and measurement PTES data to be.

The measured and calculated flowrates have been adapted, such that they respect mass balance and not flow balance. Values for 1 h timestep data are obtained from averaged 10' values, for temperatures, heat flux and flowrates. When, within the same hour-timestep, water has both been coming into and out from the same pipe, then the difference between inlet and outlet flowrates is assumed to calculate inlet or outlet flowrates.

For lid losses, knowledge of the cover thickness (0.240 m) and the insulation material conductivity (0.04 W/m/K) were used, together with top and bottom lid temperature sensors measurements to calculate the lid heat flux using: $\varphi = -\frac{\lambda_{insulation}}{t_{lid}} \Delta T$, where φ is the lid heat flux through the lid, in W/m^2, $\lambda_{insulation}$ is the insulation thermal conductivity in W/m/K, t_{lid} is the lid insulation thickness, and ΔT is the temperature difference between the top and the bottom of the PTES insulation.

Energy content of the PTES is calculated from knowledge of the temperature distribution, placement of the temperature sensors, PTES geometry, and by assuming a constant water mass of 58'330 ton (60'000 m^3 at 80°C). The internal energy change is then calculated by subtracting energy content at the end of the year with energy content at the beginning of the year.

Based on the calculated internal energy change, the inlet/outlet heat balance and the calculated lid losses, bottom & sides heat losses are calculated:

$$Q_{bottom-sides} = Q_{lid-losses} + Q_{in/out} - Q_{internal\ energy\ change}$$

2.1.3 Modelling approach

When planning pit thermal energy storage (PTES) projects, it is necessary to model accurately the operation of the PTES within the energy system where it should be integrated in order to evaluate the feasibility of the project. Such modelling can be performed in the simulation environment TRNSYS, which has been used by PlanEnergi to model projects involving PTES for the past 15 years.

TRNSYS is a complete and extensible simulation environment for the transient simulation of energy systems. It is used by engineers and researchers around the world to validate new energy concepts, from simple domestic hot water systems to the design and simulation of buildings and their equipment, including control strategies, occupant behavior, renewable energy systems (wind, solar, photovoltaic, hydrogen systems), etc.

A TRNSYS project is typically setup by connecting components graphically in the program called 'Simulation Studio'. Each Type of component is described by a mathematical model in the TRNSYS simulation engine and has a set of matching Proformas in Simulation Studio. The proforma has a black-box description of a component: inputs, outputs, parameters, etc. TRNSYS components are often referred to as 'Types' (e.g. Type 1 is a solar collector). In the present report, 3 different Types representing PTES are used and calibrated.

2.1.3.1 Presentation of the 3 PTES components

TRNSYS offers 3 components possibilities to model a PTES. The simplest one is called the 'XST model' (TRNSYS Type 342), developed by TransSolar. This model assumes that the storage has a cylindrical shape with vertical walls (see left part of Figure 2.11). This model is 1-dimensional for the water layers and 2-dimensional for the soil, as it assumes full rotational symmetry of the storage and the surrounding ground layers, which makes it fast to calculate.

Recently, two other and more sophisticated TRNSYS model components for modelling PTES have been developed. One of these is the "truncated cone" model (TRNSYS Types 1300 and 1301 combined), developed by Natural Resources Canada and TESS. This model assumes that the storage has the shape of an inverted truncated cone (see central part of Figure 2.11). It is composed of two TRNSYS components: one for modelling the water part of the storage itself (Type 1300) and one for modelling the surrounding soil (Type 1301). The interactions between the storage and the soil are modelled by connections between these two components. This model (like the XST model) 1-dimensional for the water layers and 2-dimensional for the soil (full rotational symmetry of the storage and the surrounding ground layers).

The other recently developed TRNSYS component for modelling PTES is the "truncated pyramid" model (TRNSYS Type 1322), developed by TESS, exclusively for PlanEnergi and SOLITES. This model assumes that the storage has the shape of an inverted truncated pyramid (see right part of Figure 2.11), as is more or less the case with all Danish PTES to date. This model is 1-dimensional in modelling the storage itself (it models the water as multiple layers of equal thickness) but 3-dimensional in modelling the surrounding ground layers. This model is the most sophisticated PTES model currently available for TRNSYS and fits best to the usual PTES geometry found in Denmark. It does, however, have longer calculation times than the XST model and the truncated cone model, especially when the truncated pyramid model is set to model the storage and soil in high resolution.

All three TRNSYS components assume that the PTES is divided into 16 to 64 isovolumic and isothermal horizontal layers (called "Nodes") that exchange heat with one another. The PTES has a constant volume during the simulation (no evaporation, no filling or emptying) and constant physical properties (density, thermal conductivity, etc.). A graphical representation of the model geometry is shown in Figure 2.12 with an example of 4 Nodes. D_{depth} is the depth between storage top and soil surface in case it is buried, R_{top}/R_{bot} are respectively the radius of the PTES top and bottom surface (for Type 1300 – 1301), R_{ext} is the insulation extension length, while R_{far} and D_{deep} are the far field and deep earth distances (over which no heat transfer is considered). For Type 1322, it's not one but two parameters that are used for each length dimension (length and width), but the same set of parameters are used. For instance, R_{top} is replaced by L_{top} and W_{top}, respectively length and width of the top of the PTES.

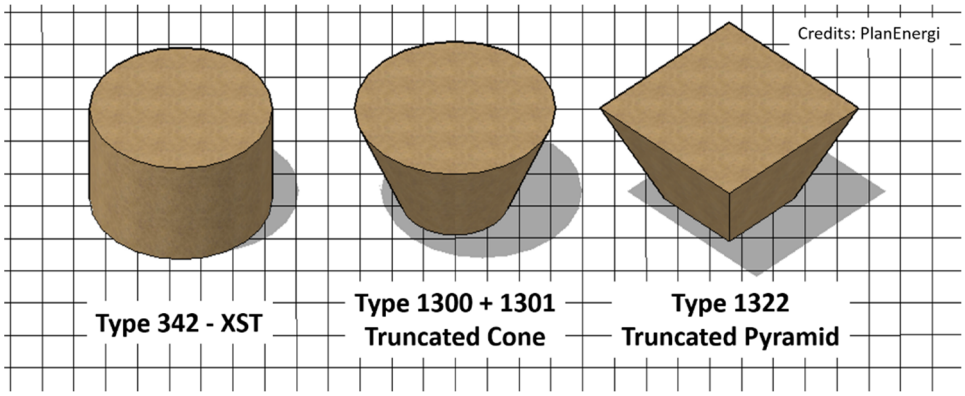

Figure 2.11. Geometry used for the three PTES components in TRNSYS: Type 342 (left), Type 1300 + Type 1301 (middle) and Type 1322 (right).

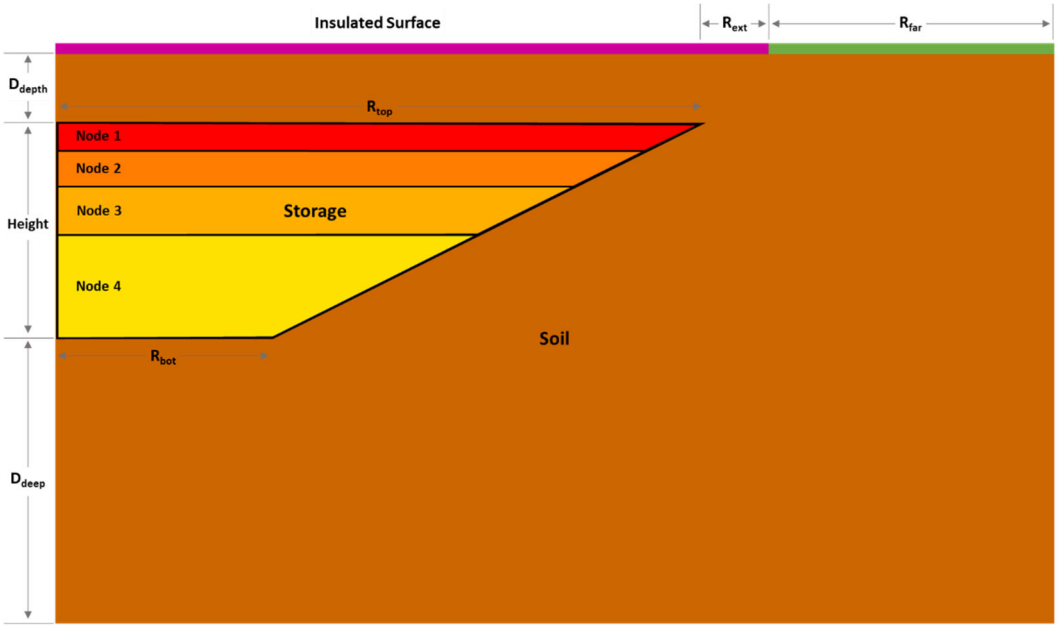

Figure 2.12. Geometry and main parameters used for Type 1300 + 1301 (and Type 1322).

2.1.3.2 Presentation of the calibration model & method

In this report, these three TRNSYS PTES components (Types 342, 1300+1301 and 1322) are calibrated using measurement data from the PTES in Dronninglund in Denmark. The calibration is performed with data for the whole year 2017 in a resolution of 10 minutes. The measured input temperatures and flows etc. for the Dronninglund storage are given as input data to the PTES models, and the resulting calculated output temperatures, flows etc. from the simulation are then compared to the corresponding measured data. In this way, the performance of the three different TRNSYS PTES components in emulating the operation of the Dronninglund storage can be evaluated and compared. This provides information on which of the models is most suitable for modelling PTES (measured on accuracy, calculation time etc.) and how large the deviation between modelled PTES and measurement PTES data are expected to be.

The graphical layout of the TRNSYS model that was constructed for the calibration is shown in Figure 2.13. The model only consists of a heat supply from an undefined source and a heat load to an undefined sink, with the PTES located in between (thick red/pink/blue lines). The measurement data from Dronninglund is used as inputs for the heat supply and heat load that connect to the PTES. No other components, such as heat exchangers, heat pumps, etc. are included in the model, because the aim of this model is to evaluate the performance of the PTES module only. The model also plots and prints the results (dotted orange lines), calculates the error (the deviation in the model results from the measurement data, green lines) and summarizes the annual performance (by means of the integrator, brown lines).

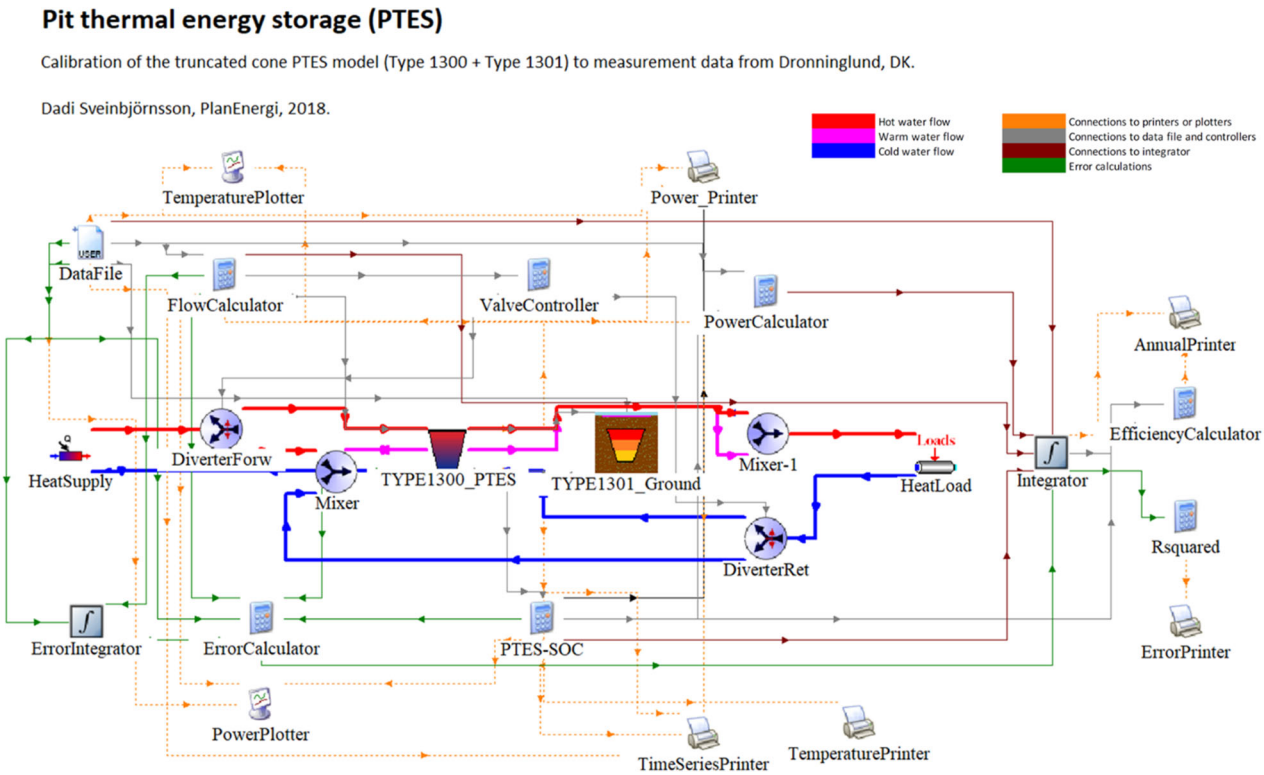

Figure 2.13. TRNSYS model layout used for the PTES calibration, here with the truncated cone PTES component implemented (Type 1300 + Type 1301).

The TRNSYS model exists in three versions, for calibration of the three different PTES components. The three models are identical except for the PTES component, main difference being that the truncated cone model (Type 1300 and 1301) contains two components for the PTES, while Type 342 and Type 1322 each are contained in only one component.

2.1.3.3 Calibration of the PTES components

Each of the three TRNSYS model versions furthermore exists in several variations, where values for some model parameters are varied between scenarios. The following parameters are varied:

- Calculation time step: 10 min. or 60 min.
- Number of tank segments: 32, 16 or 64 (is only varied for the XST model – Type 342)
- Lid and bottom insulation loss coefficient (or thermal conductivity)
- Soil calculation delay (this parameter only exists for the truncated pyramid model – Type 1322, it corresponds to the interval between each calculus of the soil temperature distribution)
- Size of smallest nodes (parameter for Type 1301 and Type 1322) for the soil modelling
- Number of years calculated[5]
- Initial ground and initial storage (water) temperature

The TRNSYS model version with the XST PTES component exists in six variations, the model version with the truncated cone PTES component also exists in six variations, and the model version with the truncated pyramid PTES model exists in seven variations.

The PTES input parameters calibrated in each variation, as well as some other key model parameters, are shown in Table 2.2, Table 2.3 and Table 2.4. The model calculates the operation of the storage for 1 to 3 years, and only the results for the last calculation year are presented in this report.

[5] When more than one year is calculated, the same dataset (from 2017) is re-used as input for each year.

Two key parameters were kept constant across models and models variations, to be coherent with the actual geometry of the PTES (see main parameters gathered in Table 2.1). These parameters are:

- The storage volume. This is directly related to the fact that the thermal capacity of the storage is proportional to the storage volume, following the equation (in the case of a PTES, where heat is stored mostly in the water):

$$PTES_{capacity} = \rho_{water} V_{storage} cp_{water} \left(T_{storage}^{max} - T_{storage}^{min}\right)$$

  where ρ_{water} is the water density in kg.m^{-3}, $V_{storage}$ is the storage water volume in m^3, cp_{water} is the water thermal conductivity in J.kg^{-1}.K^{-1}, and $T_{storage}^{max,min}$ is the maximum (respectively minimum) temperature reached inside the storage.
- The storage lid area, because the heat losses through the lid are the most important losses in the PTES (compared with losses to the side or the bottom of the PTES).

In order to respect these design parameters, the storage height is varied in the different models to obtain the same storage volume according to the different geometries.

Table 2.2. Variations of calibration parameters for Type 342.

Parameter	Unit	342_1	342_2*[6]	342_3*	342_4*	342_5	342_6
Calculated years	years	3	3	1.08[7]	1.08[7]	1.08[7]	1.08[7]
Time step	minutes	10	10	10	60	60	60
Tank segments	-	32	32	32	32	64	16
Volume	m^3	60’000	60’000	60’000	60’000	60’000	60’000
Storage height	m	7.345	7.345	7.345	7.345	7.345	7.345
Lid area	m^2	8’170	8’170	8’170	8’170	8’170	8’170
Insulation thickness	cm	24	24	24	24	24	24
Insulation conductivity**[8]	kJ/(hr·m·K)	0.1667	0.1105	0.111	0.1103	0.1103	0.1103
Side fraction of insulation**	-	0	0	0	0	0	0
Bottom fraction of insulation**	-	0	0.3775	0.4625	0.6400	0.6400	0.6400
Initial ground surface temperature**	°C	10.8	84.25	43.8	35.5	35.5	35.5
Initial water temperature**	°C	10	64.5	37.25	37.5	37.5	37.5

[6] Each variation marked with a star * is the result of a calibration. The other model variations either use design parameters or reuse the calibrated parameters from another variation.
[7] 1.08 years corresponds to 1 year preceded with 1 month of pre-filling of the PTES at the initially measured top/middle/bottom temperatures, as the detailed start temperature isn’t available for Type 342.
[8] Each parameter marked with a double star ** is calibrated with GenOpt.

Table 2.3. Variations of calibration parameters for Type 1300 + Type 1301.

Parameter	Unit	1300_1	1300_2*	1300_3*	1300_4*	1300_5	1300_6
Calculated years	-	1	1	1	3	1	1
Time step	minutes	10	10	60	60	60	60
Tank nodes	-	32	32	32	32	32	32
Size of smallest node	m	2	2	2	2	0.25	10
Volume	m^3	60'000	60'000	60'000	60'000	60'000	60'000
Storage height	m	16	16	16	16	16	16
Lid area	m^2	8'170	8'170	8'170	8'170	8'170	8'170
Top loss coefficient**	kJ/(hr·m^2·K)	0.6	0.47	0.47	0.47	0.47	0.47
Edge loss coefficient (for all nodes)**	kJ/(hr·m^2·K)	2.4	3.92	3.7	11.1	3.7	3.7
Bottom loss coefficient**	kJ/(hr·m^2·K)	2.4	17.2	16.8	16.1	16.8	16.8
Initial ground temp.**	°C	10.8	20	23.5	69.9	23.5	23.5
Initial water temp.**	°C	measured[9]	measured	measured	69.8	measured	measured

Table 2.4. Variations of calibration parameters for Type 1322.

Parameter	Unit	1322_1	1322_2*	1322_3	1322_4	1322_5	1322_6	1322_7*
Calculated years	-	1	1	1	1	1	1	1
Time step	minutes	60	60	60	60	60	60	10
Tank nodes	-	32	32	32	32	32	32	32
Soil calculation delay	hours	24	24	24	48	6	24	24
Size of smallest nodes (soil, tank & corner)	m	2	2	0.25	2	2	10	2
Scalar for nodes (soil, tank & corner)	-	2	2	2	2	2	2	2
Volume	m^3	60'000	60'000	60'000	60'000	60'000	60'000	60'000
Storage height	m	16	16	16	16	16	16	16
Lid area	m^2	8'170	8'170	8'170	8'170	8'170	8'170	8'170
Top loss coefficient**	kJ/(hr·m^2·K)	0.6	0.475	0.475	0.475	0.475	0.475	0.5
Edge loss coefficient (for all nodes)**	kJ/(hr.m^2·K)	2.4	3.65	3.65	3.65	3.65	3.65	2.8
Bottom loss coefficient**	kJ/(hr·m^2·K)	2.4	17.25	17.25	17.25	17.25	17.25	8
Initial ground temp.**	°C	10.8	23.75	23.75	23.75	23.75	23.75	15.25

2.1.4 Calibration results

TRNSYS calculates for each timestep the energy balance for the system, in this case for the PTES component. Figure 2.14 to Figure 2.16 represent the water temperature variations inside the PTES for the different TRNSYS Types, and Figure 2.17 to Figure 2.19 show curves representing measured heat inlet/outlet and lid losses evolution next to heat inlet/outlet and lid losses modelled by TRNSYS.

[9] The temperature is given for each node of Type 1300 based on start measured PTES temperatures.

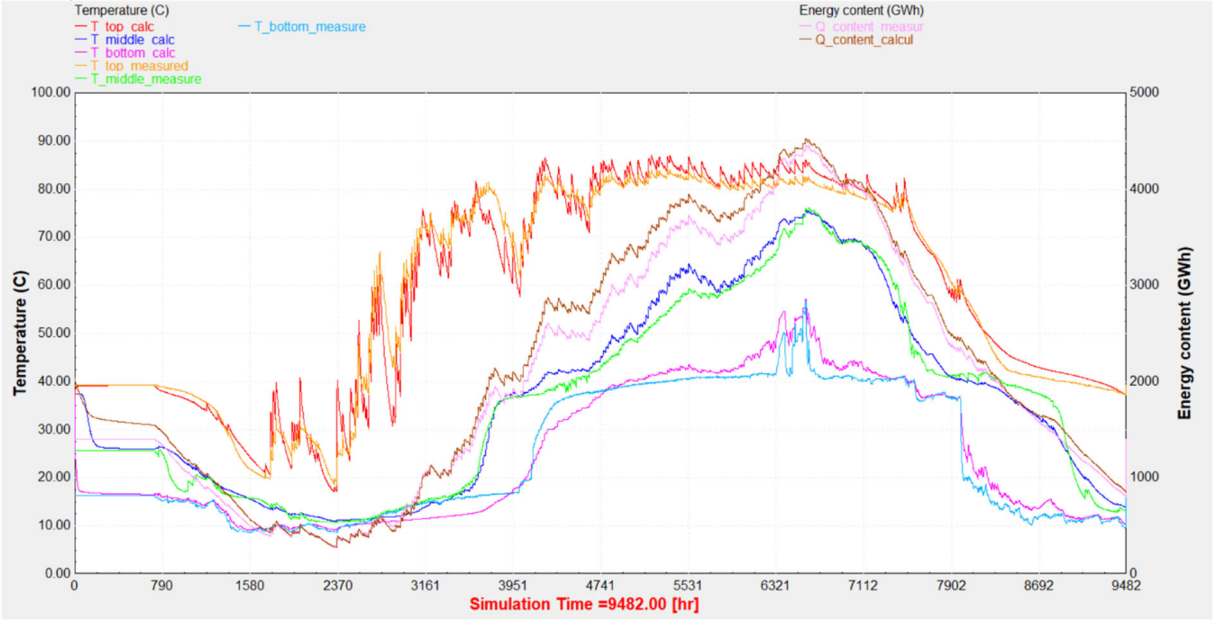

Figure 2.14. Temperature distribution inside the PTES as modelled by TRNSYS (Type 342).

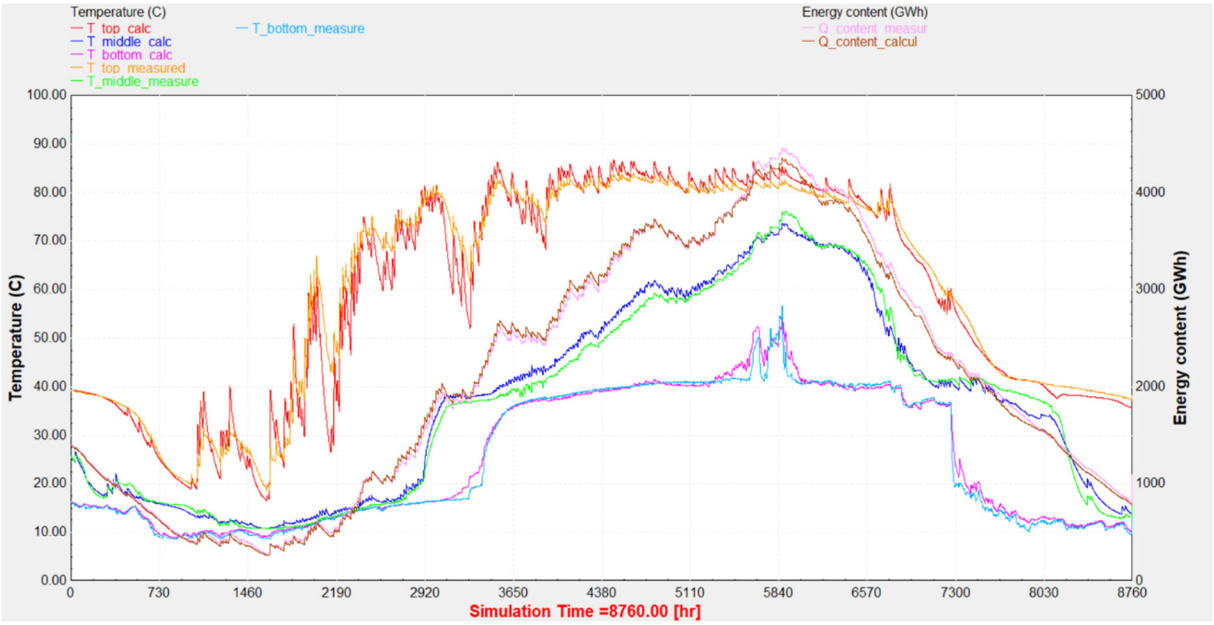

Figure 2.15. Temperature distribution inside the PTES as modelled by TRNSYS (Type 1300 + Type 1301).

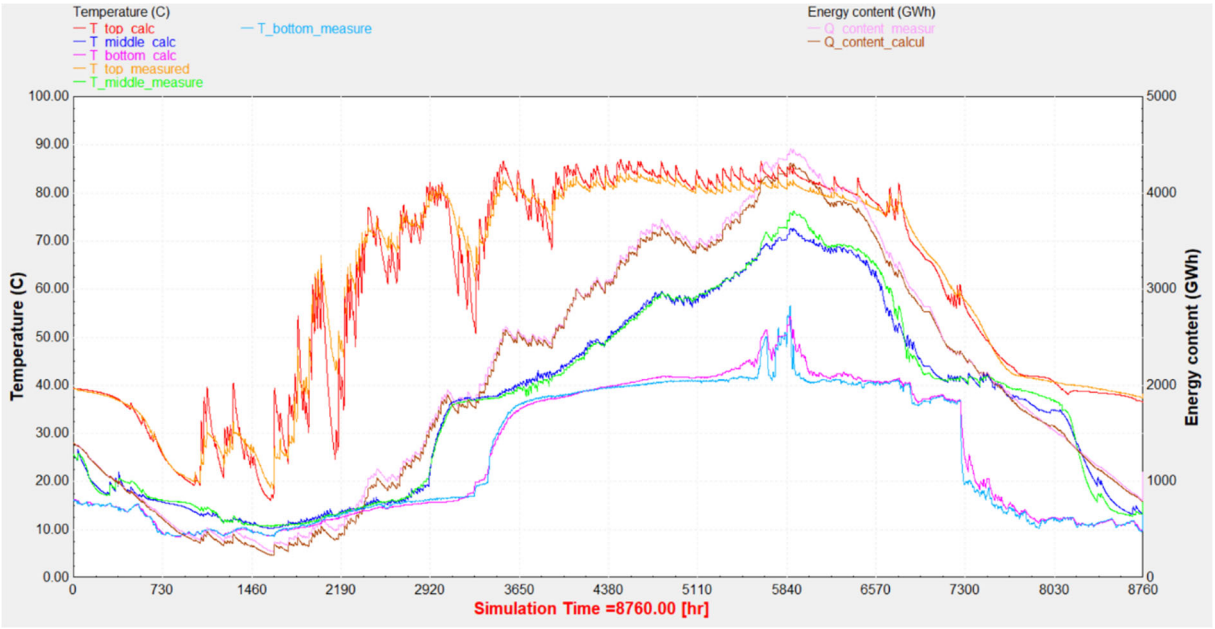

Figure 2.16. Temperature distribution inside the PTES as modelled by TRNSYS (Type 1322).

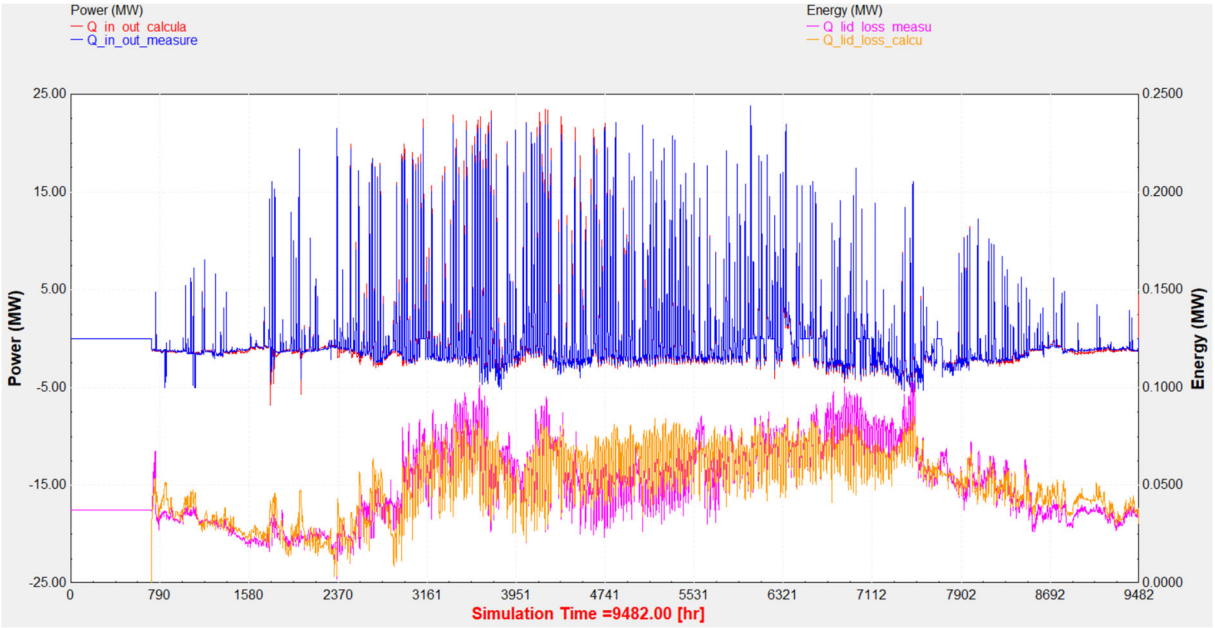

Figure 2.17. Curves representing measured heat inlet/outlet and lid losses evolution next to heat inlet/outlet and lid losses modelled by TRNSYS (Type 342).

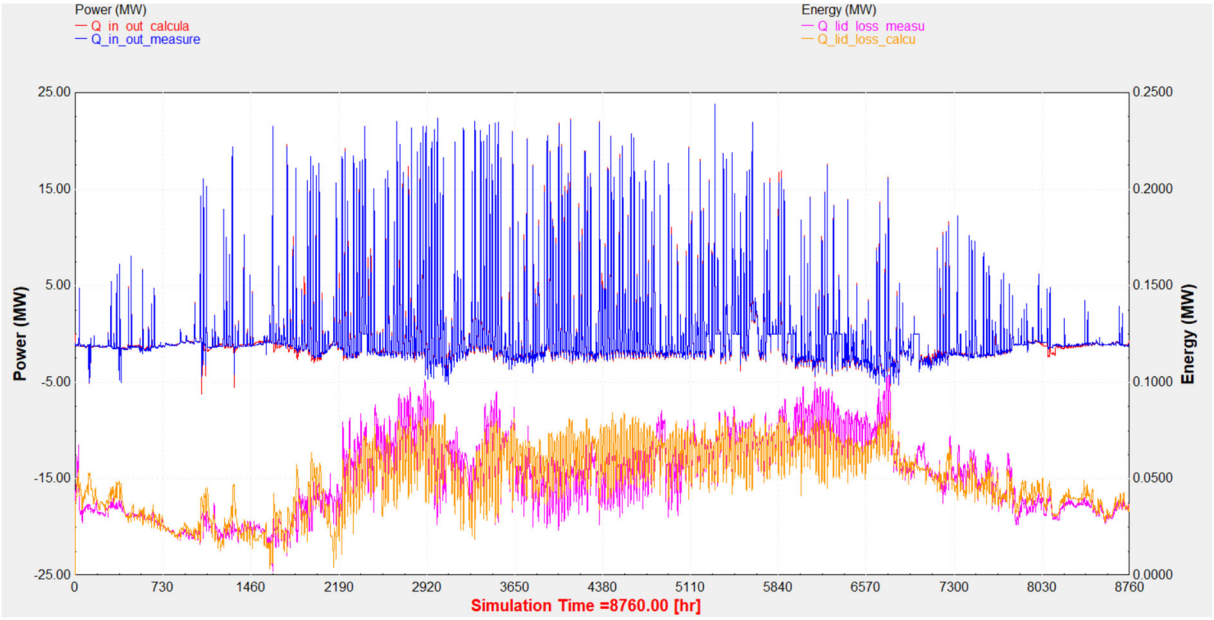

Figure 2.18. Curves representing measured heat inlet/outlet and lid losses evolution next to heat inlet/outlet and lid losses modelled by TRNSYS (Type 1300 - 1301).

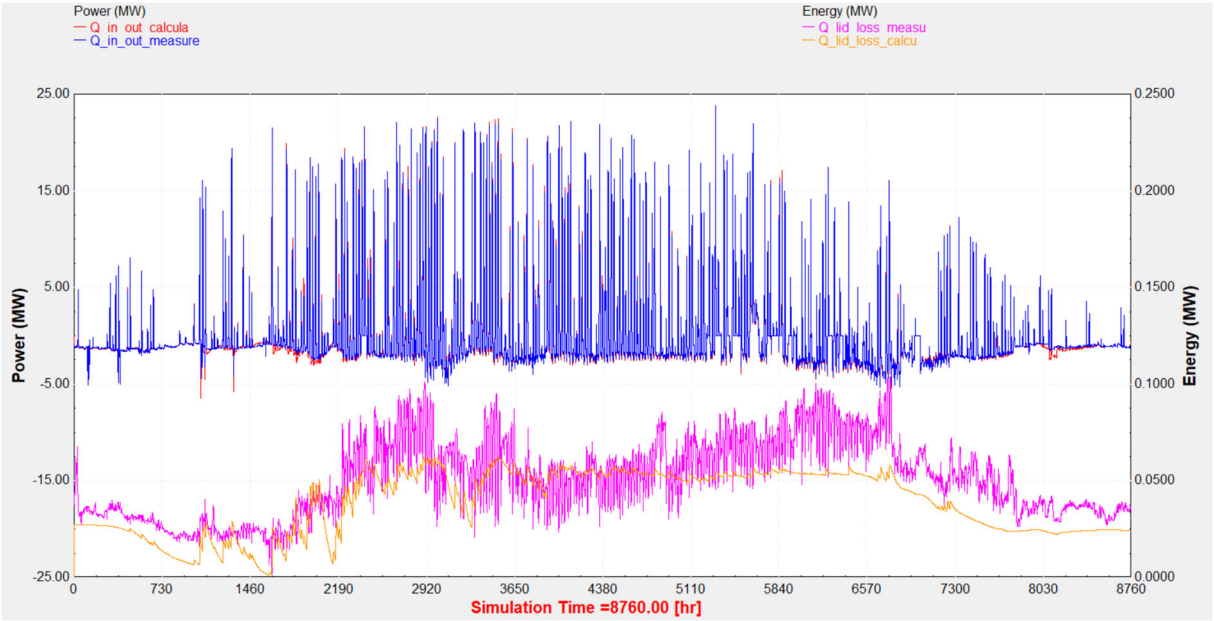

Figure 2.19. Curves representing measured heat inlet/outlet and lid losses evolution next to heat inlet/outlet and lid losses modelled by TRNSYS (Type 1322).

2.1.4.1 Methodology – Coefficient of determination (R^2)

The results of the TRNSYS PTES component calibration are shown in Figure 2.20 to Figure 2.32. Figure 2.20 and Figure 2.21 show the prediction accuracy of the model, for the different PTES components (Type 342, 1300+1301 and 1322) and for the different model variations. The coefficient of determination (R^2) is used as a measure for the model accuracy (see explanation in the following paragraphs). This quantifies how well the model fits to the measurement data on a 10-minute (or 60-minute) resolution basis, over the course of a whole year.

The coefficient of determination is a method of quantifying how much of the variance in the measurement data is captured (or predicted) by the modelled data. For a vector y containing measurement data and a vector f containing the modelled data, the coefficient of determination is defined as:

$$R^2 = 1 - \frac{S_{res}}{S_{tot}}$$

where S_{res} refers to the "residual sum of squares" defined as:

$$S_{res} = \sum_i (y_i - f_i)^2$$

and S_{tot} refers to the "total sum of squares" in the measurement data (which is proportional to the variance in the measurement data):

$$S_{tot} = \sum_i (y_i - \bar{y})^2$$

with $\bar{y}$ mean value of the measured data, defined as:

$$\bar{y} = \frac{1}{n}\sum_i y_i$$

and i corresponds to the i[th] timestep in the simulation, where the total number of time steps per year are either 52'560 (for a 10-minute resolution) or 8'760 (for a 60-minute resolution). f_i is the calculated data for that timestep.

The coefficient R^2 takes on values between 0 and 1, where a value of 1 means that the model perfectly captures the variance in the measurement data (i.e. that the model yields a perfect prediction of the measurement data). As an example, for $R^2 = 0.95$, 95% of the variance in the measurement data has been accounted for in the model, and 5% has not been accounted for.

For each PTES model, the loss coefficients, the initial ground temperature and the loss coefficients for the top, side and bottom of the PTES are varied to obtain best total coefficient of determination:

$$R^2{}_{total,PTES} = \frac{R^2{}_{top\_temp.} + R^2{}_{middle\_temp.} + R^2{}_{bottom\_temp.} + R^2{}_{Q\_in} + R^2{}_{Q\_out} + R^2{}_{lid\_losses}}{6}$$

The optimization program *GenOpt* was used to perform the calibration and is used to find the set of parameters that maximizes $R^2{}_{total,PTES}$.

In the following section, coefficients of determination are presented for top, middle and bottom temperatures, as well as energy inlet, energy outlet and energy losses through the lid. A last coefficient is presented, the global coefficient of determination, defined by:

$$R^2{}_{global,PTES} = \frac{R^2{}_{top\_temp.} + R^2{}_{middle\_temp.} + R^2{}_{bottom\_temp.} + R^2{}_{Q\_in} + R^2{}_{Q\_out}}{5}$$

This new coefficient was used to exclude the lid losses from the comparison between models. Indeed, lid losses are the least reliable measurements from the list and using them could make it seem like a less accurate model performs better, simply because its lid losses oscillate just as much as the measurements.

2.1.4.2 Results presentation – model prediction accuracy

In terms of model accuracy, two main parameters have been analyzed:

- Key temperatures inside the PTES (top, bottom and middle temperatures, corresponding to the heights of the diffusors presented in Table 2.1)
- Energy balance from inlet/outlet of water, and energy losses through the lid

For each type of TRNSYS PTES model, a color code has been used. Shades of blue have been used for Type 342, shades of pink/orange/brown for Types 1300 & 1301, and finally shades of green for Type 1322 (see Figure 2.20 for an example). A darker shade of a given color simply indicates a higher model variation number.

Reference data is displayed using black bars.

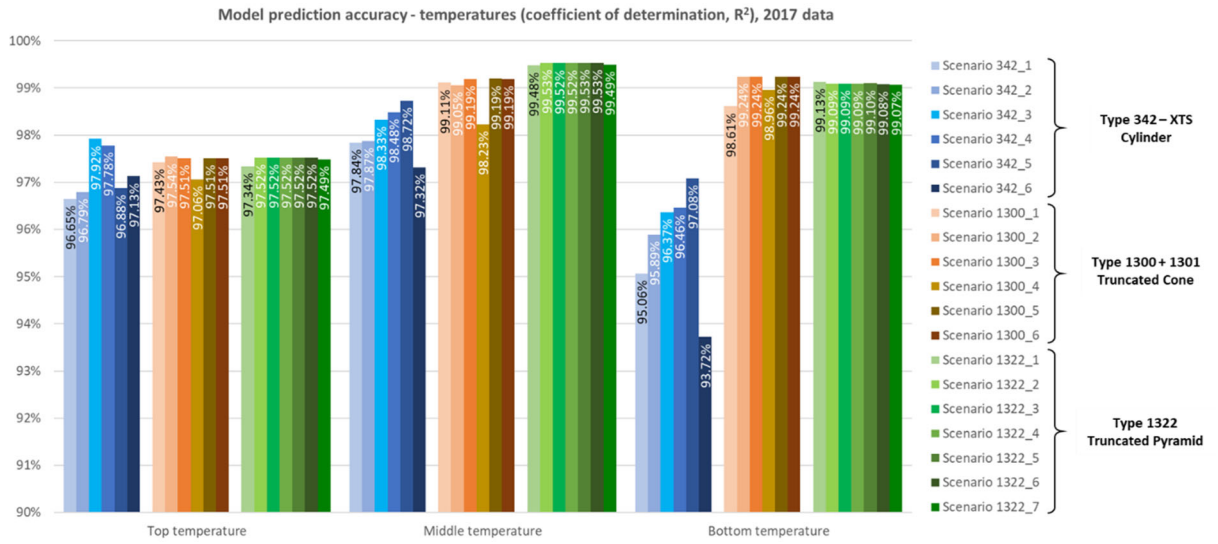

Figure 2.20. Model prediction accuracy for the calibration scenarios of all PTES models, shown in terms of the coefficient of determination (R^2), for temperatures.

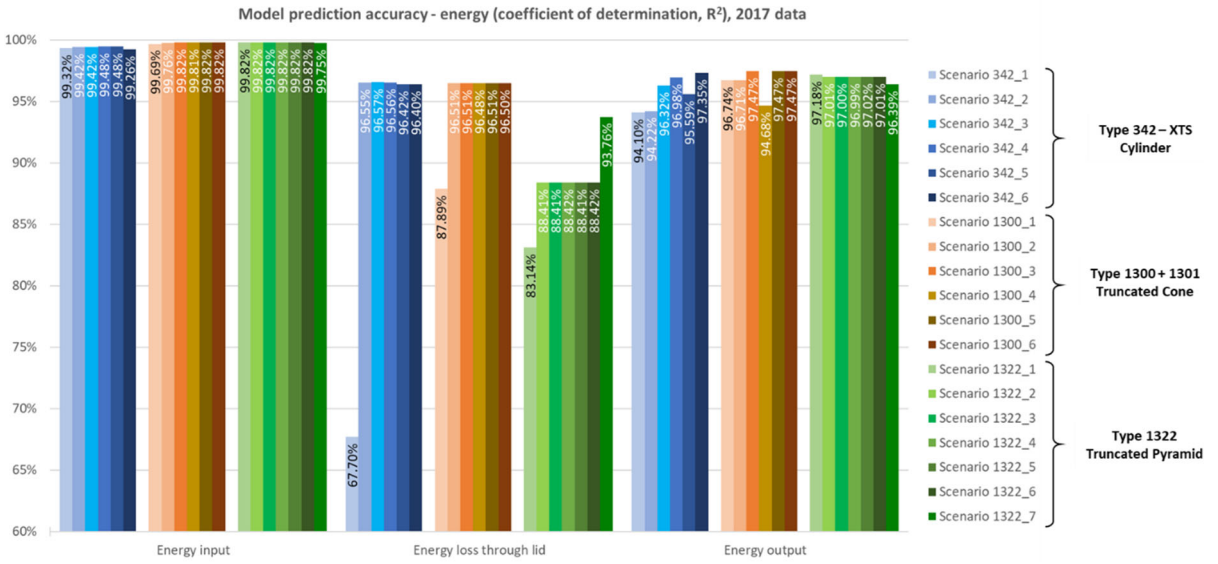

Figure 2.21. Model prediction accuracy for the calibration scenarios of all PTES models, shown in terms of coefficient of determination (R^2), for energy balances (input/output) and lid losses.

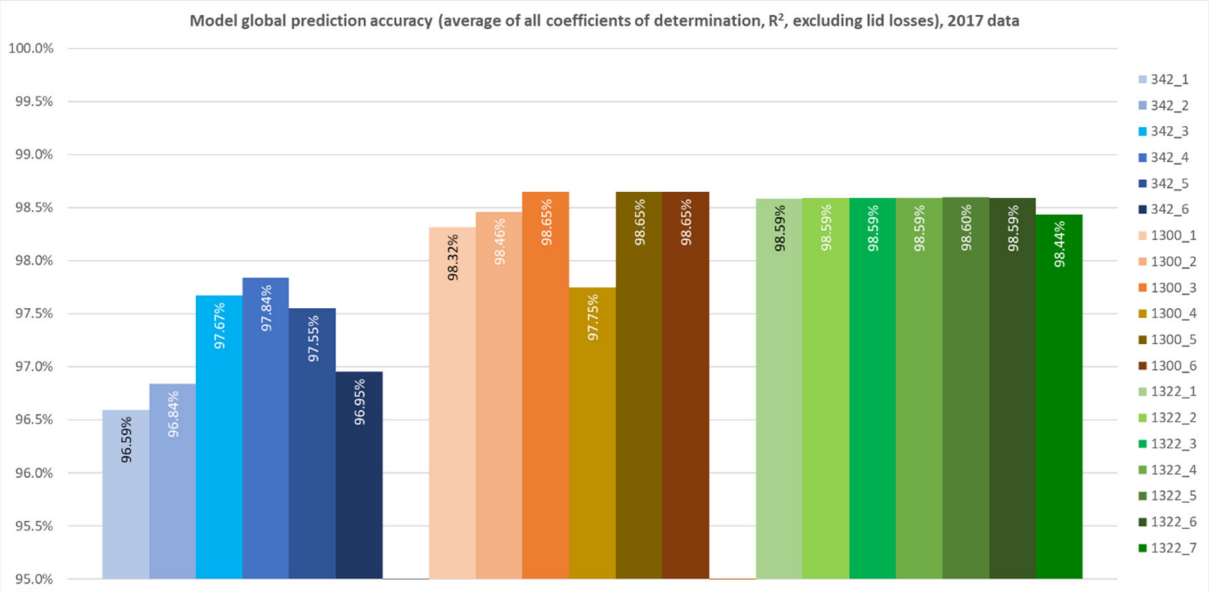

Figure 2.22. Global model prediction accuracy for the calibration scenarios of all PTES model variations, calculated from the average of all coefficients of determination (R^2) regarding temperatures, energy input & output, but excluding lid losses.

2.1.4.3 Results presentation – annual energy balance and storage performance

Besides the model accuracy, another determining factor for evaluating how well a model can reproduce an actual system, is by comparing annual performance of the PTES. Since both 10 minutes and 60 minutes timesteps datasets have been studied, different reference measurement data have been used, and the following results present the results from each dataset separately. The difference comes mostly from the fact that the 60 minutes dataset was obtained by calculating averaged values of the 10' dataset for every hour.

In this section, annual values are compared for: energy input into the PTES, energy output from the PTES, energy losses through the lid of the PTES, energy losses through the bottom & sides of the PTES, internal energy change, number of storage cycles per year realized by the PTES, and storage efficiency for the PTES.

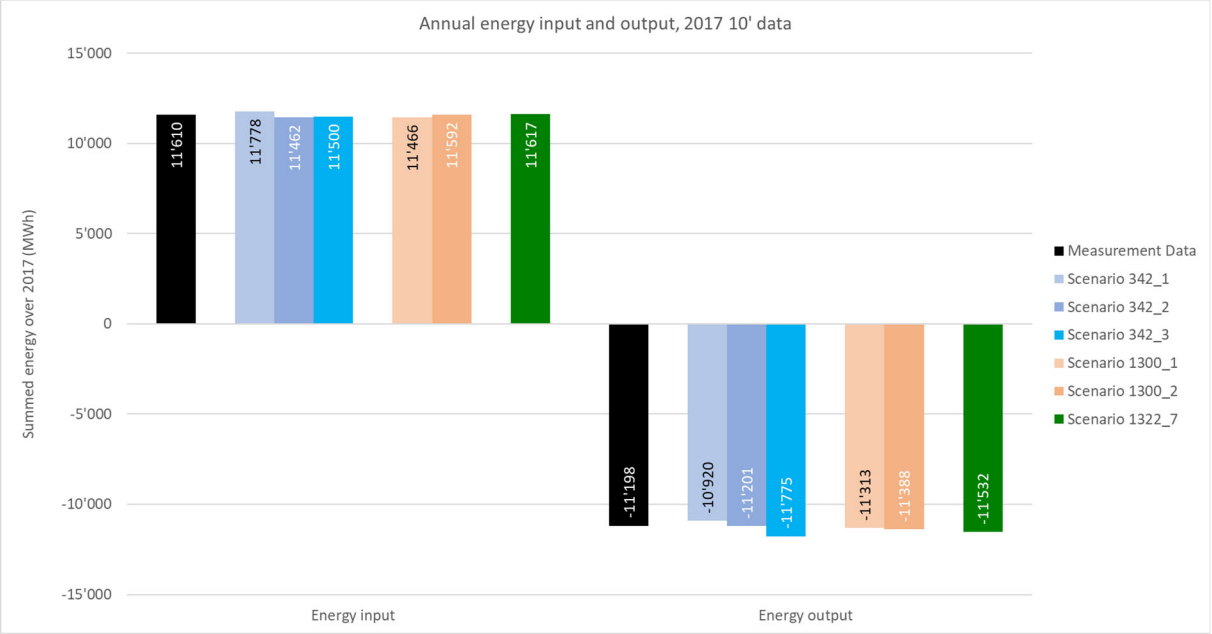

Figure 2.23. Annual energy input and output of the PTES models, with 10' data. The black column shows the measurement data, to which the model results can be compared. All values are in MWh.

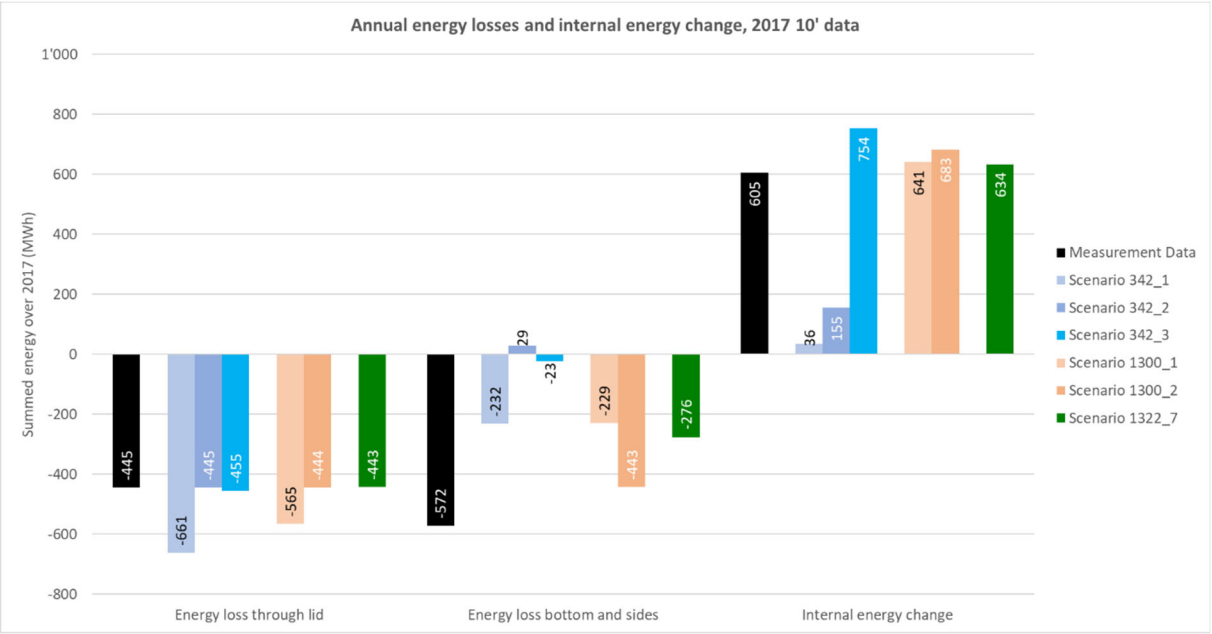

Figure 2.24. Annual energy losses through the lid, through the bottom & sides together with the internal energy change of the PTES models, with 10' data. The black column shows the measurement data, to which the model results can be compared. All values are in MWh.

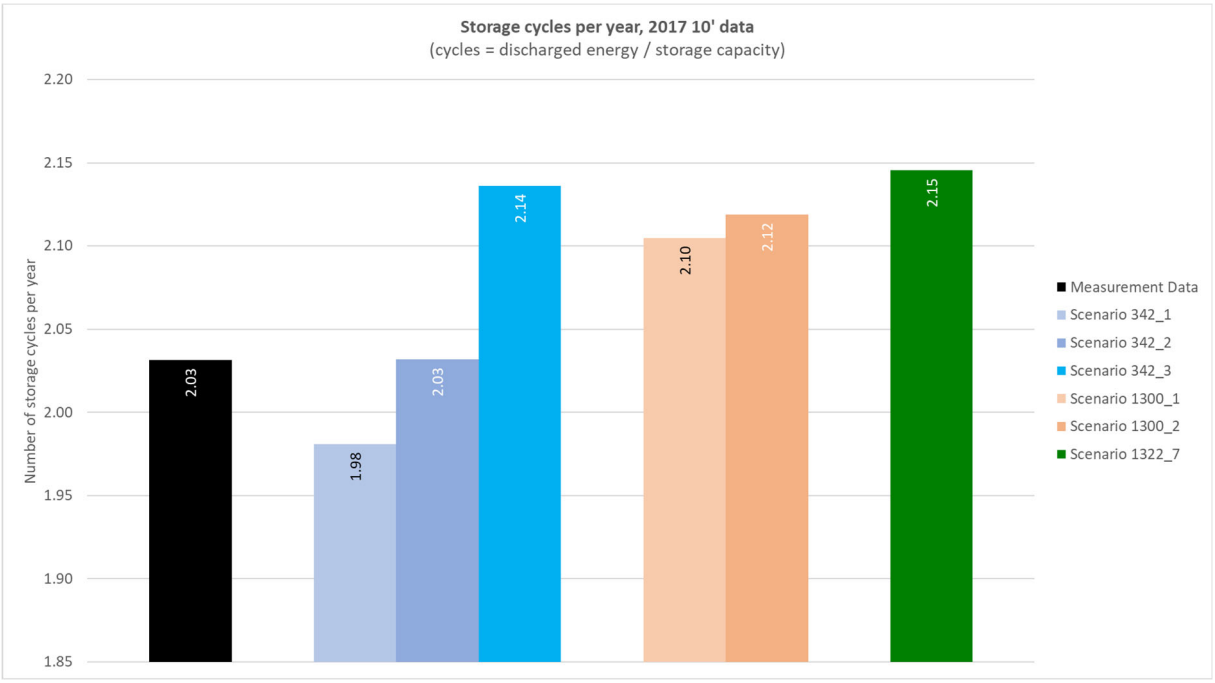

Figure 2.25. Number of storage cycles per year, with 10' data. The black column shows the measurement data, to which the model results can be compared.

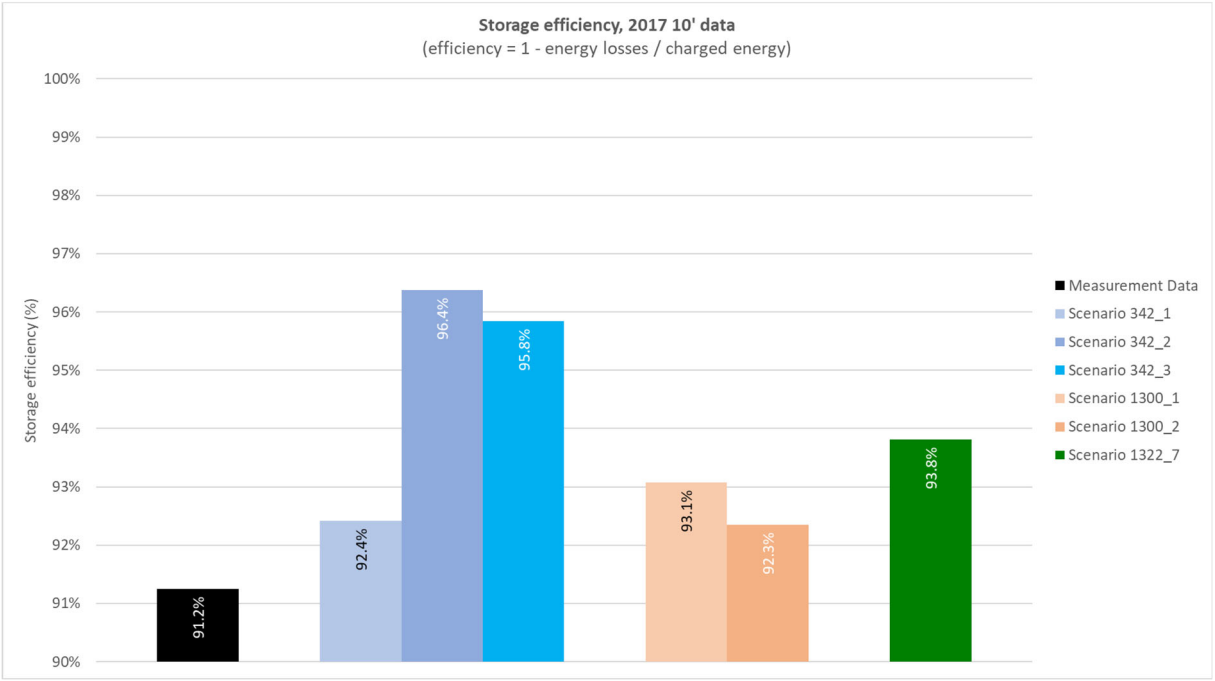

Figure 2.26. Storage efficiency over the last year of simulation, with 10' data. The black column shows the measurement data, to which the model results can be compared.

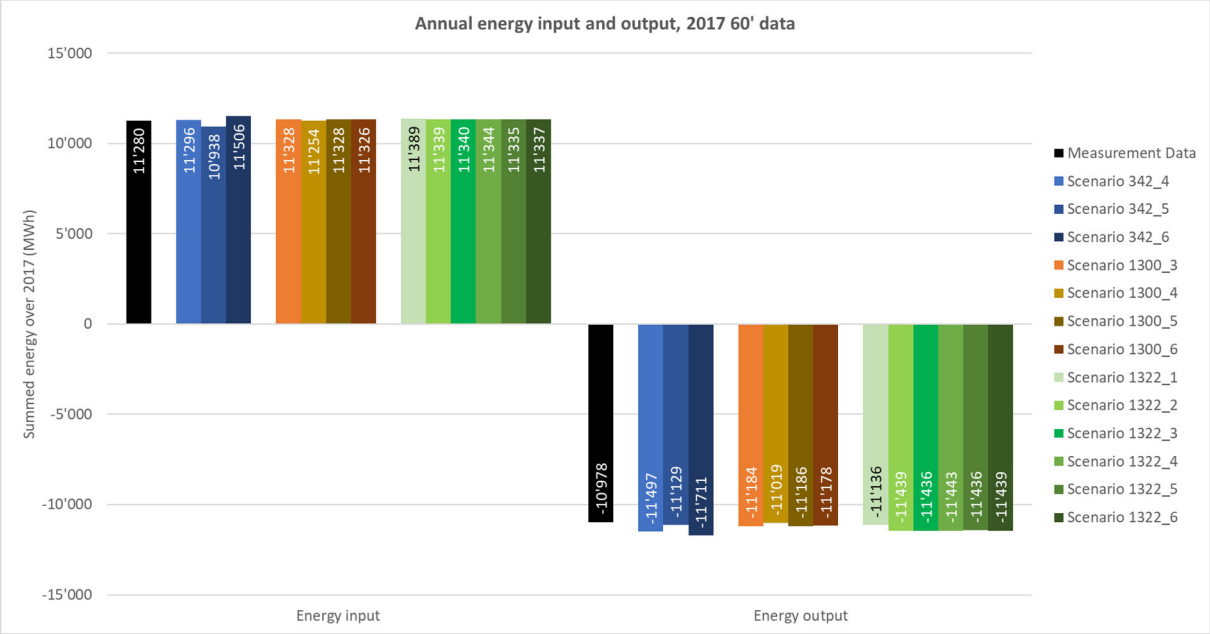

Figure 2.27. Annual energy input and output of the PTES models, with 60' data. The black columns shows the measurement data, to which the model results can be compared. All values are in MWh.

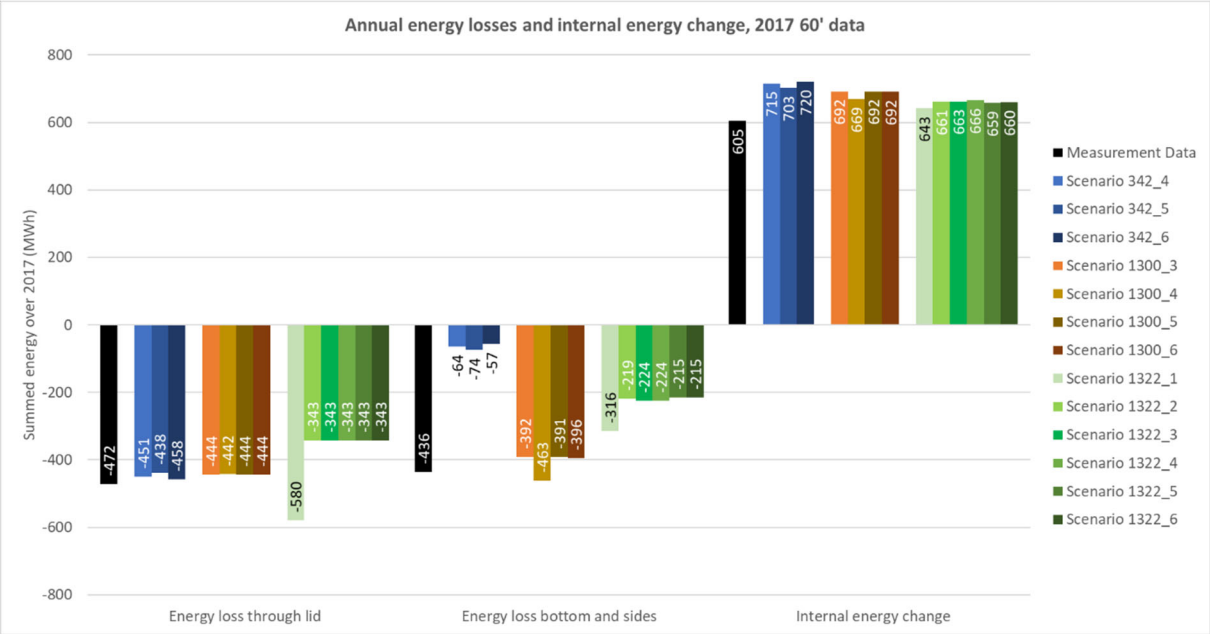

Figure 2.28. Annual energy losses through the lid, through the bottom & sides together with the internal energy change of the PTES models, with 60' data. The black column shows the measurement data, to which the model results can be compared. All values are in MWh.

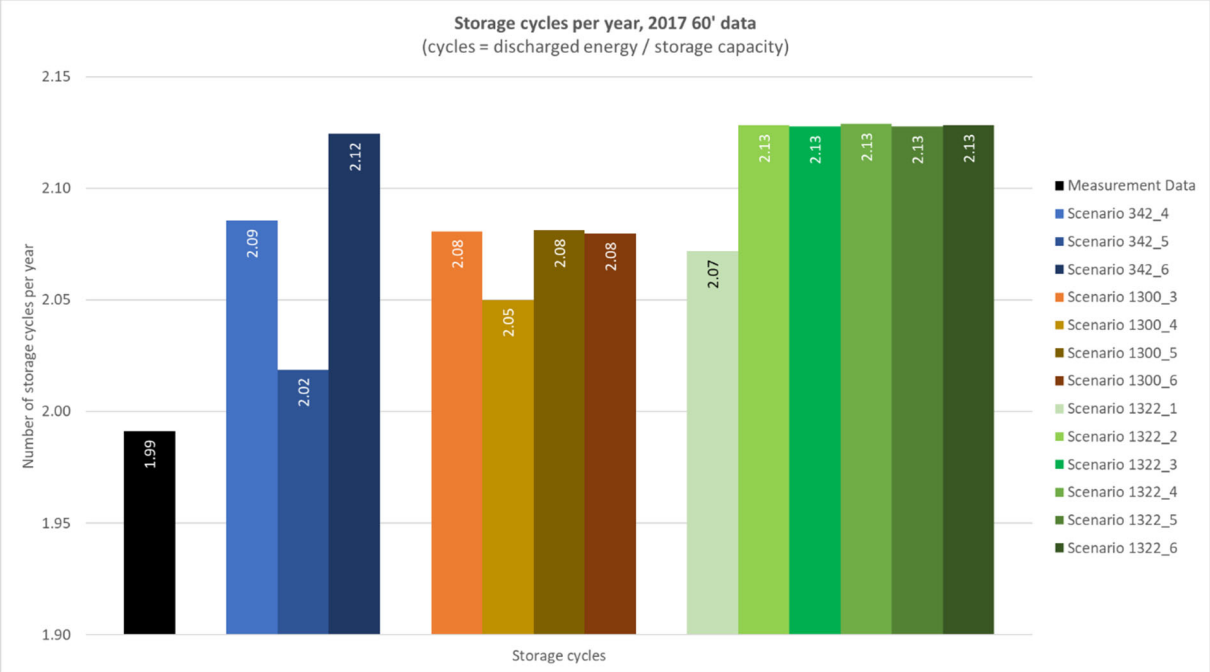

Figure 2.29. Number of storage cycles per year, with 60' data. The black column shows the measurement data, to which the model results can be compared.

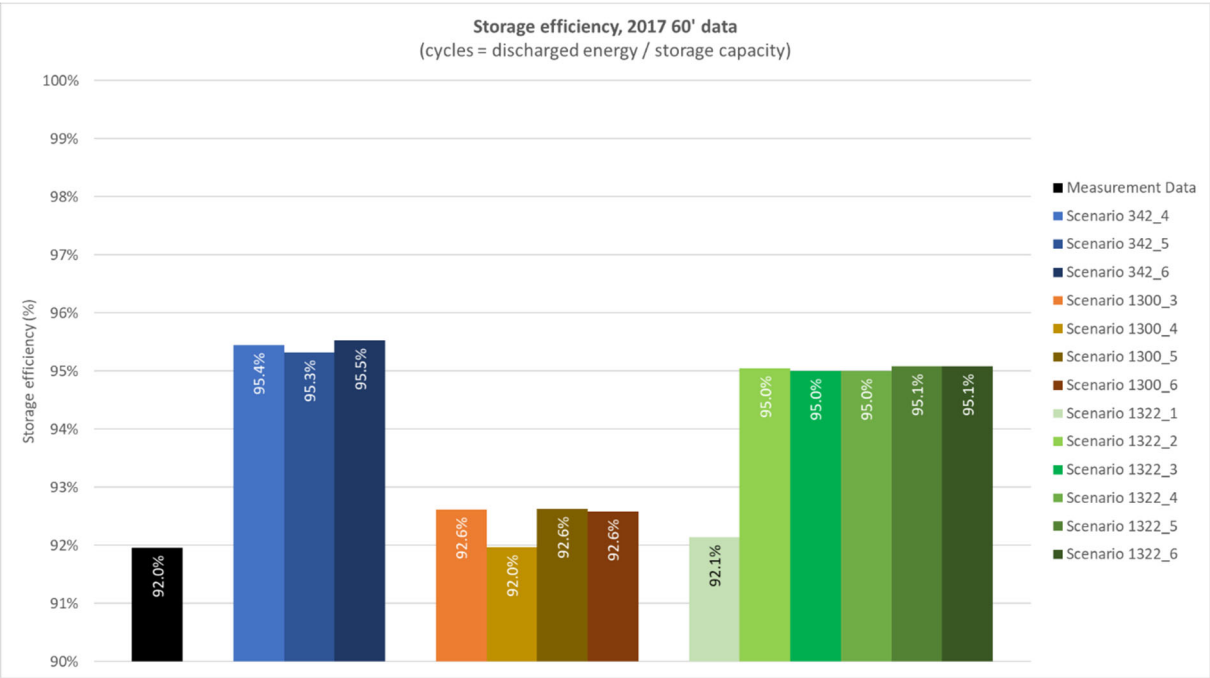

Figure 2.30. Storage efficiency over the last year of simulation, with 60' data. The black column shows the measurement data, to which the model results can be compared.

2.1.4.4 Results presentation – calculation time

In addition to these results, the calculation time was compared for the different model variations, in order to see what the computational costs were for increasing modelling accuracy.

Two ways of looking at calculation time have been studied: total calculation time and equivalent calculation time per timestep. Results are shown in Figure 2.31 and Figure 2.32.

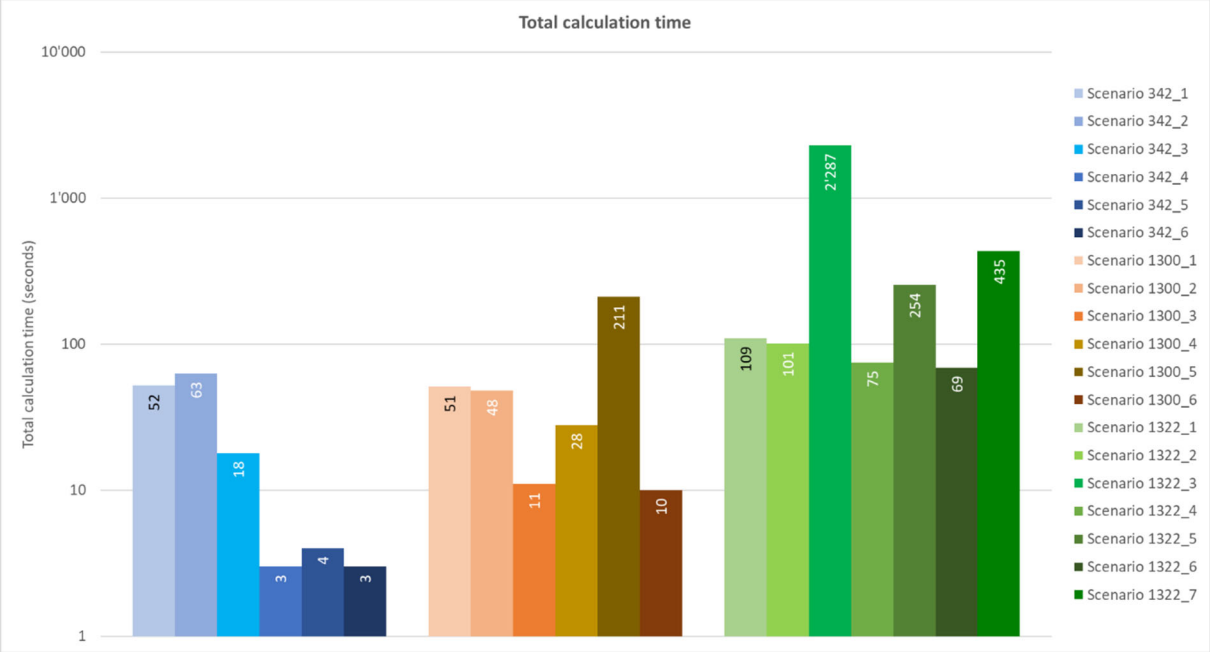

Figure 2.31. Required total calculation time for the models (for one to three-year calculation).

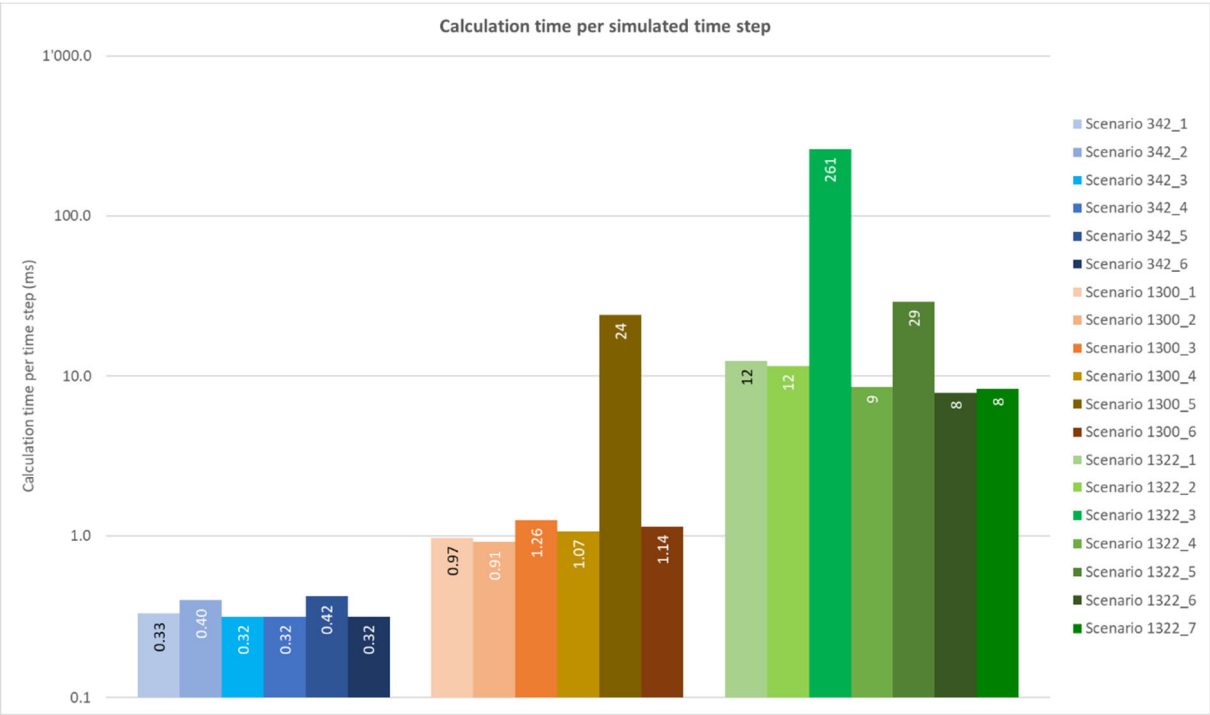

Figure 2.32. Required calculation time per calculated timestep for the models.

2.1.4.5 Results analysis

With all models, good accordance between temperature measurements from Dronninglund and the calculations has been found. Highest accuracy for the PTES top temperature is achieved by model 342_3 and the best models from Types 1300-1301 and 1322 provide similar accuracy (over 97.5%). For PTES

middle temperature, model 1322_5 provides best accuracy followed close by model 1300_3, while model 342_5 provides the best accuracy for Type 342. For bottom PTES temperature, it is model 1300_3 that provides best accuracy, followed by 1322_1, and Type 342 is behind with model 342_5. For energy input, all models are quite accurate with over 99%, and highest accuracy is provided by Types 1300-1301 and 1322, while model 342_5 is the best within Type 342 models. For energy output, the best variation of each model provides similar accuracy, just over 97%.

For the lid losses, we can see the effect of calibrating: a low initial R^2 when using design parameters is turned into higher accuracy after calibration of the loss coefficients for all 3 models. Surprisingly, the least accurate model (after calibration) regarding lid losses is the one using Type 1322, while this Type is well performing over temperatures and inlet/outlet energy balance. This can be explained by:

- the way lid losses have been measured, i.e. on a single point of the insulation, for a square shaped 8'350 m^2 lid, and then global lid losses are deduced by assuming an homogeneous heat loss through the lid, it has been observed that these losses aren't the same everywhere at the surface of the PTES
- the way lid losses are calculated in the model, i.e. by taking a constant thermal conductivity and thickness for the lid insulation, where in practice this insulation has a thermal conductivity that varies with temperature and humidity content

For energy losses through the lid, Type 342 provides the best accuracy, followed close by Type 1300-1301 and over 96% accuracy. This parameter is the only one where Type 1322 falls behind (best accuracy achieved by model 1322_7, with close to 94%). It was therefore chosen not to take this parameter into account to calculate the global accuracy of the different models.

Figure 2.19 illustrates the high precision of lid heat flux (losses) calculated (yellow line) compared with the more fluctuant lid heat flux measured (pink line) and could be the reason for lower accuracy compared with measurements for this TRNSYS model.

For global accuracy, models 1300_3, 5 and 6 provide the best results with 99.65%, followed closely by model 1322_4 with 99.60% (see Figure 2.22). The best model using Type 342 is model 342_4 with 97.84%. These results are coherent with the fact that models using Types 1300-1301 and 1322 use a geometry close to the actual PTES geometry, and the reason for Type 1322 to be less accurate can simply be explained by the fact that measurement data isn't precise nor complete enough to be compared with this very precise component.

In all cases, changing from 60' timesteps to 10' timesteps doesn't improve the model accuracy or the annual results, probably because 60' values are averaged values compared with 10' values. Using smaller node sizes or more water tank nodes doesn't significantly improve the model accuracy either. Same type of explanation there: the measured data provided lacks precision, and therefore using more precision in the model doesn't lead to much better results. Only exception to this is found for lid losses for model variation 1322_7. For this TRNSYS Type 1322, 10' values provide the best accuracy regarding lid losses (see Figure 2.21).

The fact that bottom and side heat losses are estimated indirectly (by an energy balance) makes it difficult to calculate annual losses accurately. Indeed, during operations of the PTES in Dronninglund, there has been a leakage, as well as water evaporation, and these aren't used for the calculations as they haven't been measured. Since the model doesn't calculate evaporation either, it is difficult, even for the most accurate model, to estimate very closely the annual internal energy change.

Nevertheless, one result appears clearly: calculating one year with appropriate initial conditions (pre-fill for Type 342, initial water temperature distribution for Types 1300-1301 and 1322) provides much better results than calculating 3 years with regards to internal energy change accuracy. Refer to scenarios 342_1, 342_2 and 1300_4 in Figure 2.24 and Figure 2.28.

Regarding computational time, Figure 2.32 displays clearly that Type 342 is the fastest per timestep, while Type 1322 is the slowest. Type 1300-1301 is somewhere in between.

Since all PTES models give quite accurate results with regards to heat balance and temperature distribution, and Type 342 is faster than the other models by at least a factor 3, then it would be recommended to do pre-feasibility studies with this component.

When needing to do more detailed feasibility studies, since Type 1300 is already more accurate, while remaining much faster than Type 1322, then this type would be recommended for these kinds of studies.

Type 1322 should be used for detailed studies of comparison between measurements and calculations, provided enough measurement points are available for the studied PTES, and with a high enough precision. Otherwise it could be a waste of computational power and time. Further research with more complete and accurate data should be conducted in order to confirm this last conclusion.

It is worth mentioning here that, when launching calculations without calibration (with design parameter values), Types 1300-1301 and 1322 provide better results than Type 342, especially for lid losses (see 342_1, 1300_1 and 1322_1 on Figure 2.21 and Figure 2.22). Type 1300-1301 should therefore be highly recommended for feasibility studies, where local soil and weather conditions are known.

2.1.4.6 Future improvements

For further improvements with these kinds of studies, the present report clearly shows where some improvement could be done in having an even better compliance between measurements and calculations. Some recommendations could be:

- instead of one set of measurements, have some sort of validation measurements (double probes placed at strategical places inside the PTES, around the lid, and in the ground around the PTES). This would probably be highly beneficial for lid losses measurements and calculations.
- set up a more thorough set of measurements. In the present study, the high uncertainty regarding bottom and side losses comes from the lack of data measurements to evaluate these heat transfers, as well as uncertainty on lid losses, no information about how much heat and water mass is lost through evaporation, leakage and filling of the PTES, etc. Another example is the air temperature: in the dataset used, the temperature measured at the top of the isolation is used for top insulation temperature, calculation of lid heat losses and surface temperature for the soil, where it could have been better to have an independent air temperature measurement to use as surface temperature for the soil and the lid.
- ideally, have complete data of several years in a row, to account for internal energy change, change in soil temperatures over the years, etc. In the present study, best results were obtained from 1-year calculations with proper initial conditions (temperature distribution inside the PTES on day 1 of 2017, or pre-filling of the PTES). With data from 2016 and 2015, it would have been possible to make calculations from real data over 3 years and obtain even more accurate results for 2017.
- have more probes where most of the energy content of the PTES is, which is at the top of the PTES, because of the inverted truncated pyramid geometry but also because of higher temperatures at the top. A recommendation could be to follow the isovolumetric segmentation of the PTES, as used by the TRNSYS model, instead of placing the probes every 0.5 m inside the PTES.
- for three pipes connected to the PTES, all possible flow paths can be modelled by using 6 sets of fixed couples (inlets, outlets), called “Ports” in TRNSYS:
    - (top inlet, bottom outlet)
    - (top inlet, middle outlet)
    - (middle inlet, bottom outlet)
    - (middle inlet, top outlet)
    - (bottom inlet, top outlet)
    - (bottom inlet, middle outlet)

  and by combining these Ports, it is possible to reconstruct all possible measured flow paths at any given moment through the PTES. Unfortunately, Types 1300 and 1322 only allow for 5 Ports maximum, which means that one of the Ports needs to be replaced by a combination of 2 Ports. For example, if we decide to model the PTES without using the (middle inlet, top outlet) Port, then whenever this flow path is supposed to be used, it is replaced by (middle inlet, bottom outlet) + (bottom inlet, top outlet). This doesn’t provide the same heat inlet/outlet balance, because the water transits through the top of the PTES, and for each timestep, the outlet temperatures are calculated based on heat balance, which means that the water leaving the top of the PTES and sent to the top of the PTES again will have a different temperature from the current timestep PTES top water temperature. Thus, the inlet/outlet heat balance won’t be equal to zero. Another recommendation based on these considerations would be to have a TRNSYS model with the possibility for at least 6 port (for the modelling of 3 inlets/outlets pipes), and at least 12 ports, for the modelling of 4 inlets/outlets pipes.

3 Borehole Thermal Energy Storage (BTES)

3.1 Danish case study in Brædstrup

This Danish case study is that of a Borehole Thermal Energy Storage (BTES) and consists of two solar plants of 18'600 m^2 in total, two heat accumulation tanks (or buffer tanks) of 2'000 m^3 and 5'500 m^3, a 19'000 m^3 soil volume borehole storage, a 1.2 MW_{heat} heat pump and an 10 MW electric boiler. The system supplies heat to the district heating network located in Brædstrup, Denmark[10].

3.1.1 Conceptualization

3.1.1.1 UTES concept and specifications, scope and aims of the study

The BTES in Brædstrup is located next to the solar collector field and the existing District Heating Network building (DHN). The heat pump is in the new technical building (Figure 3.1).

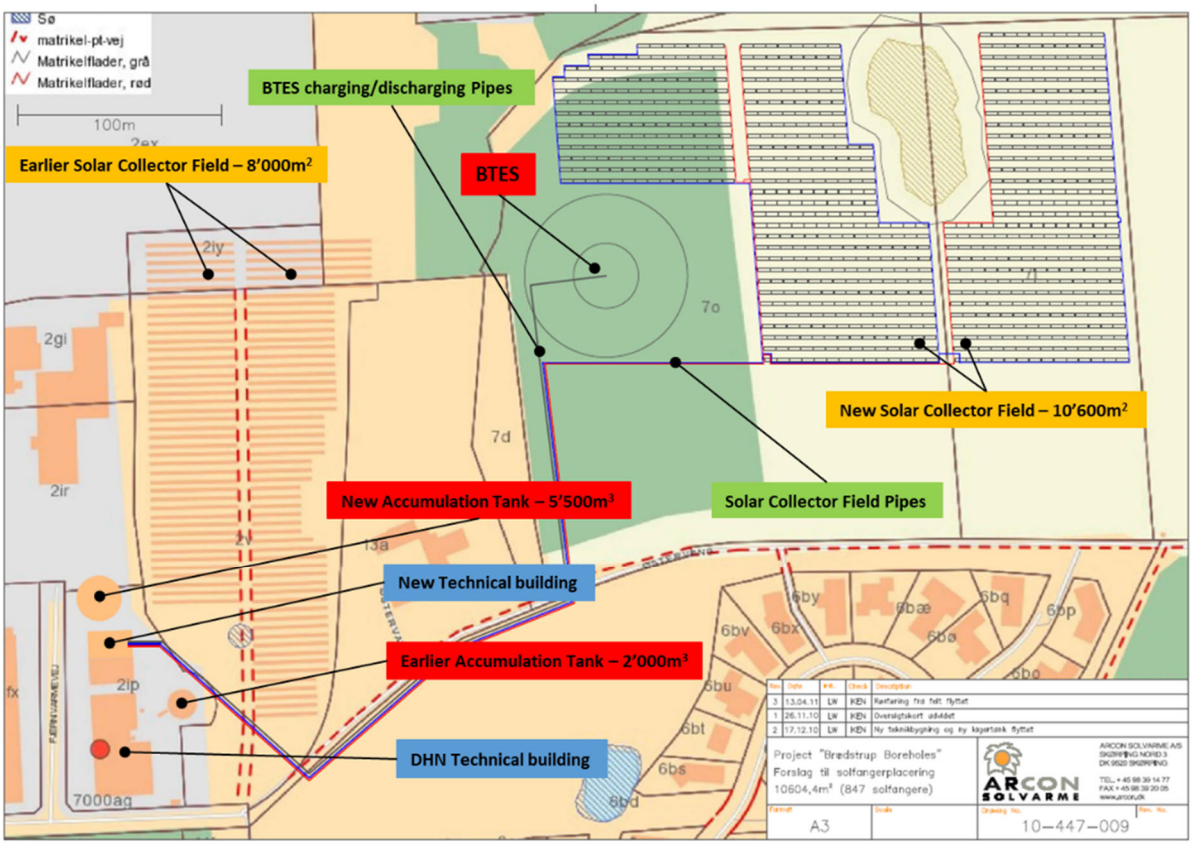

Figure 3.1. Brædstrup solar thermal production plant with seasonal thermal energy storage.

The BTES was built between 2011 and 2012, and the main characteristics are reproduced in Table 3.1, and a detailed diagram of the boreholes can be found in Figure 3.13. Pictures of the PTES while being built (Figure 3.2) and after being insulated (Figure 3.3) are shown below. The lid refers to the top insulation of the BTES.

[10] *Boreholes in Brædstrup*, 2013, EUDP project number 64012-0007-1, ForskEL project no. 2010-1-10498.

Table 3.1. Main geometry characteristics of the BTES in Brædstrup.

Parameter	Value	Unit
Volume soil	19'200	m^3
Number of boreholes	48	-
Depth of each borehole	45	m
Diameter of a borehole	15	cm
Distance between each borehole	3.0	m
Number of U-pipes per borehole	2	-
Number of U-pipes in series	6	-
Number of parallel flow strings	16	-
Diameter of the circular area with the boreholes	22	m
Insulation extension	6	m
Insulation thickness over the boreholes	0.5	m
Soil layer thickness over isolation	0.5	m
Insulation conductivity	0.12	W / (m·K)
Number of inlets/outlets	2	-

Figure 3.2. Brædstrup BTES under construction. Boreholes drilling (left) and spreading of the cockle shells insulation around the BTES well (right).

Figure 3.3. Geo textile and semi permeable roof foil placed upon cockle shells.

The BTES is insulated at the top with 2 layers of 25 cm of cockle shells, covered by 50 cm of soil. The insulation covers a diameter of 22 m (the boreholes area) and is progressively decreased to the edge of the insulation extension, 6 m away from the boreholes area border. A global cross section can be found in Figure 3.4 and a detail is shown in Figure 3.5.

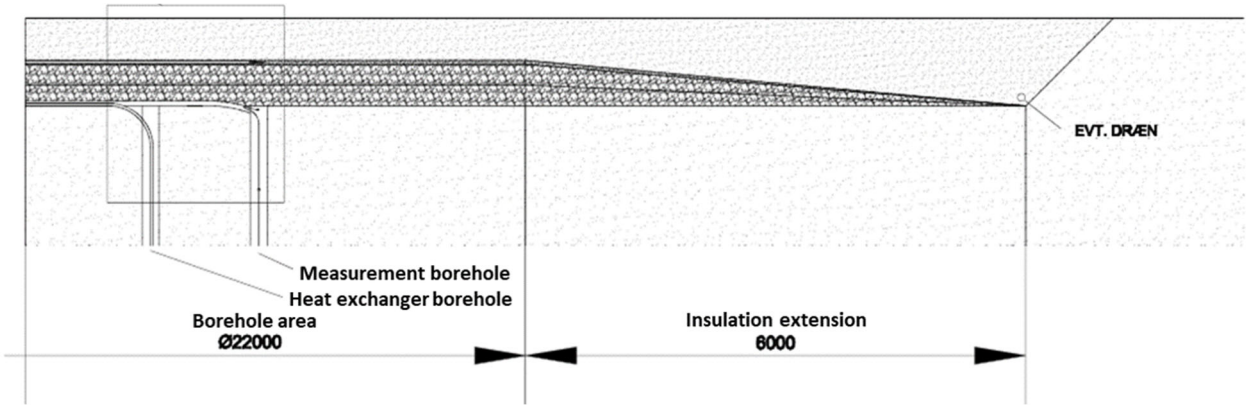

Figure 3.4. Global cross section of the BTES lid insulation.

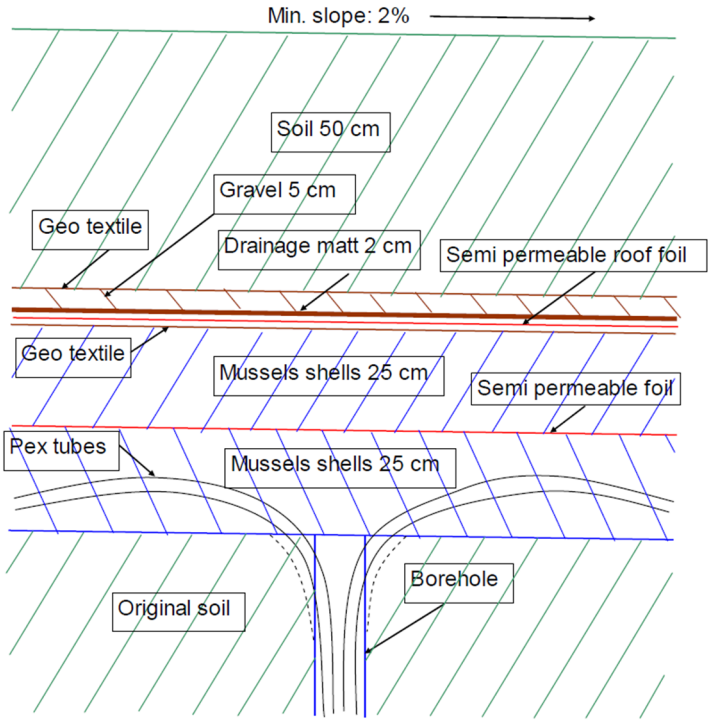

Figure 3.5. Detailed cross section of the BTES lid insulation (the implementation used cockle shells instead of mussel shells).

Thermal conductivity was tested for compressed mussel shells and evaluated for the configuration given in Figure 3.5. A resulting 0.121 W/(m·K) was estimated for mussel shells, and the same value was assumed for the cockle shells, although no measurement has been carried out again[10].

3.1.1.2 Brædstrup solar heating system concept presentation

The BTES in Brædstrup is exclusively used as a seasonal heat storage, storing heat in the summer, where solar heat production is high and heat demand from the DHN is low, and releasing this heat in the winter when heat demand is highest. Since this BTES is used for demonstration purposes, and the district heating company wants to make the best economical use of it, it is now mostly used for storing excess heat from the system that otherwise should have been blown off.

The BTES was included into the existing DHN installation, and Figure 3.6 represents the principle diagram of how it was connected to the other components (heat pump, accumulation tank, etc.).

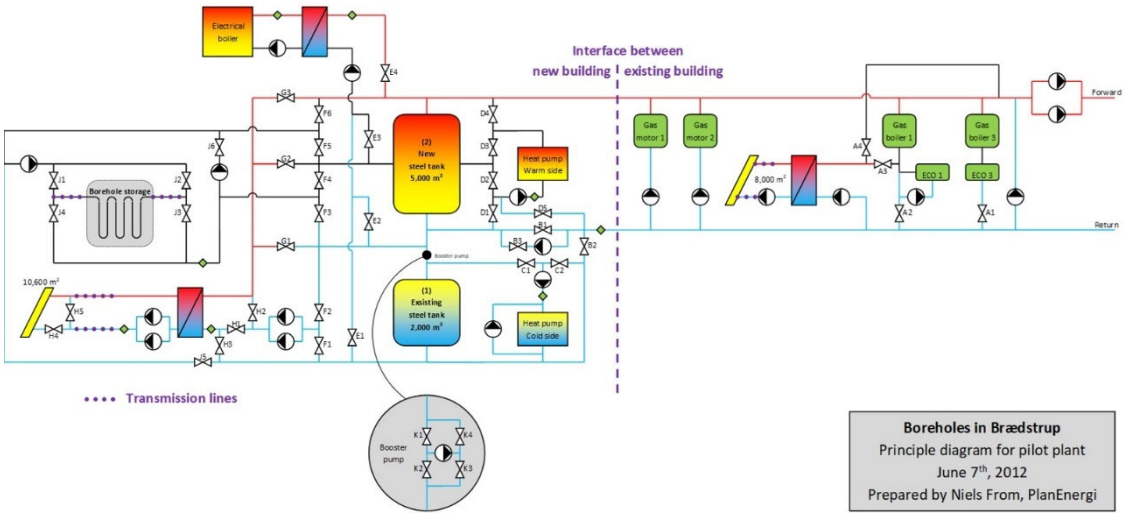

Figure 3.6. Principle diagram of the solar heating system including BTES in Brædstrup. Green squares are flow/energy meters. The diagram is simplified and not all equipment is shown.

The system was setup such that both accumulation tanks are used as a part of the solar heating system, in combination with the heat pump and the borehole storage. The booster pump (see detail at the bottom of Figure 3.6) is used to control the water level in the accumulation tanks. During winter operations, the smaller tank is used mostly for storing the cold water, while the new tank contains the hot water. In the summer, both are used equally for storing hot water for the solar collector fields.

3.1.1.3 Brædstrup solar heating system design, BTES geometry and geology

The pilot BTES was meant to be only the first step before a full-scale plant covering 50 % of the yearly heat consumption with solar energy. Therefore, the design of the pilot plant started with design of the full-scale plant including solar collectors, accumulation tank, a full-scale borehole storage and heat pumps.

In the area pointed out for new solar collectors 42'000 m^2 of solar collectors could be placed and the accumulation tank for the full-scale plant was expected to be 5'000 m^3 + 2'000 m^3. The sizing of the full-scale BTES was optimized to achieve the best (lowest) heat price, varying only BTES volume, number of boreholes and depth, charging flowrate of the BTES, charging and discharging season and amount of 1.2 MW_{th} heat pumps. Optimum solution converged for a 210'000 m^3 soil volume, 553 boreholes (45 m depth). Optimization was carried out with GenOpt using calculations carried out in TRNSYS.

In the original application for the BTES funding, the pilot project was meant for app. 8'000 m^3 soil volume, a solar thermal plant of app. 8'000 m^2, a 2'000 m^3 buffer tank and a heat pump (app. 1 MW_{heat}). With results from the full-scale optimization, initial design for the pilot BTES was evaluated around the following values:

- Solar collector area (8'000 m^2) + 8'000 m^2
- Steel tanks[11] (2'000 m^3) + 5'000 m^3
- Amount of 1.2 MW_{heat} heat pumps: 1
- BTES: 50 boreholes (1/10 of the full-scale) for 19'000 m^3 soil volume

For the full-scale BTES the optimum cross-sectional area of a single borehole was found to be approx. 7.76 m^2 (Figure 3.7). Figure 3.8 shows the shape of the cross-sectional area (in grey color) of a single borehole for 3 different borehole patterns: circular, square and triangular. The circular pattern is the ideal situation; however, this is not suited for actual implementation. Instead, a square or a triangular (i.e. hexagonal cross-section) pattern can be used.

[11] It is worth noting here that the accumulation tank volume is designed for the full-scale BTES, and thus not optimized for the pilot plant BTES.

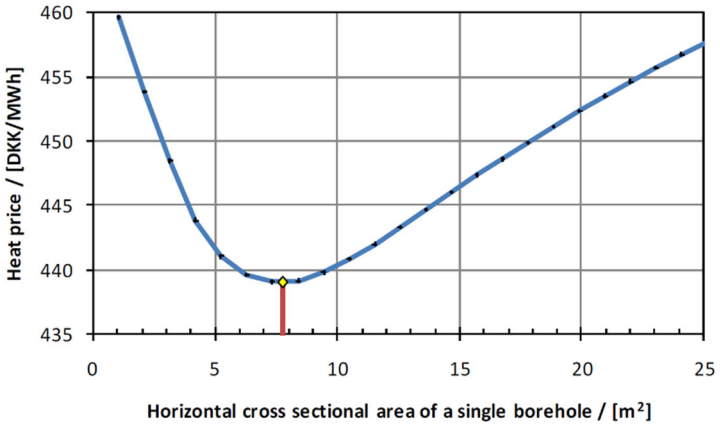

Figure 3.7. Heat price as a function of the cross sectional area of the boreholes.

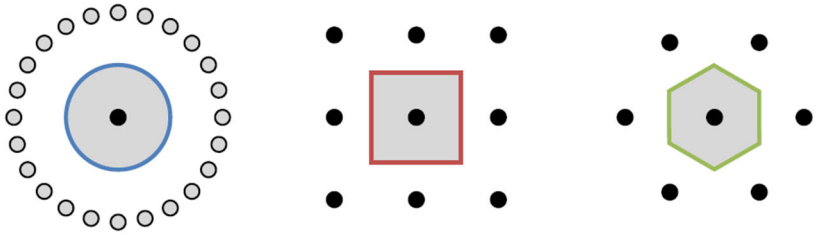

Figure 3.8. Top view of the borehole volumes for the ideal situation (circular), a square pattern and a triangular pattern.

To obtain the optimum cross-sectional area of 7.76 m^2, the distance (D) between two neighbor boreholes should be:

- For circular area: D ≈ 3.14 m
- For square pattern and area: D ≈ 2.79 m
- For triangular pattern / hexagonal area: D ≈ 2.99 m

A drilling can be deflected from the vertical line by e.g. stones. Therefore, the drilling company had stated that the minimum (safe) distance between the boreholes is 3.0 m in order to avoid damage on a finished borehole when the neighbor boreholes are drilled. With a safe distance of 3.0 m it was not possible to obtain the optimum cross-sectional area with a square pattern (because 3.0 m > 2.79 m). Choosing a triangular pattern instead, the safe distance coincidentally almost corresponds to the optimum area.

The final design will show that having 6 boreholes connected in series (see Figure 3.13) is ideal for heat exchange with a limited pressure drop of 2 bars, and therefore 48 boreholes was chosen instead of 50 (as it is a multiple of 6). With 48 boreholes, and by assuming 8 m^2 of soil around each borehole for 50 m depth (45 m + 5 m of soil depth heat up under each borehole) gives a total soil volume of 19'200 m^3.

As for the solar collector field, enough space was available for 10'600 m^2 of thermal solar collectors, and that's what was chosen to be implemented, although it is not optimized to fit the BTES volume/capacity.

In order to calibrate properly the BTES model, a geotechnical study was carried out to determine the thermal properties of the soil at the BTES site. Soundings, borings and thermal measurements were carried out. Based on the performed site investigation the company GEO recommended[10] to use the following average values in the design of a pilot energy storage with borings to 45 meters depth:

- Thermal conductivity: λ = 1.42 W/(m·K)
- Heat capacity: c = 0.9 – 1.0 kJ/(kg·K)
- Volumetric heat capacity: C ≈ 1.8 - 2.0 MJ/(m^3K)

Another important thermal property to know is that of the grouting material used. Grouting material is the filling used for each borehole. It is the environment directly in contact with the charging/discharging BTES

pipes (see Figure 3.9). Thermal conductivity of the chosen grouting material was tested in the laboratory and evaluated after 15 days of rest[10] to 1.44 W/(m·K).

Figure 3.9. Thermal tests of the grouting material.

3.1.1.4 Brædstrup solar heating system first monitoring results

Monitoring data for evaluation was available from January 2012. The new solar collector area went into operation in April 2012, and the BTES was charged for the first time in May 2012.

Simulations and operational experience of other comparable projects show that BTES have a start-up phase of about 3-5 years. In this time the ground outside the storage volume is heated up by the thermal losses from the storage. Hence, normal operation with calculated storage efficiencies and storage temperatures will not be reached in the first years of operation. Therefore, the first real system measurements including BTES were only available from 2013, and the first BTES energy flow analysis was first given from 2014 (see Figure 3.12).

The entire system monitoring heat balance for 2017 is shown in Figure 3.10. It clearly shows that the pilot BTES is small compared to the DHN system in Brædstrup, also when considering design figures for the pilot BTES. The reason for why the measurements are much lower than the design figures are mentioned in Section 3.1.1.2: after proving the concept during the first years, the BTES was only used for storing excess heat that otherwise should have been blown off. Under normal operations, using the accumulation tanks to store heat directly from the solar collectors is cheaper and provides as much heat. Also, as the solar production values show 2017 was much less sunny than the design year, which also justifies why the BTES has been used so little. Nonetheless, the solar fraction achieved for 2017 is the same as the design solar fraction of the pilot plant. This is due to the good use of the large accumulation tanks.

The overall thermal performance of the BTES for years 2014 to 2017 can be found in Figure 3.11, and the progressive decrease in BTES use can be clearly observed in Figure 3.12.

3.1.1.5 Scope and aims of the BTES measurement study

Due to operational decay of the BTES, the only data that was chosen for reference to compare with calculations are years 2014 and 2015. In order to calibrate the BTES model in TRNSYS, it has also been chosen to isolate that component from the rest of the system to study it in detail. Monitoring results (such as air temperature, inlet water temperature and flowrates) are used as inputs to the model.

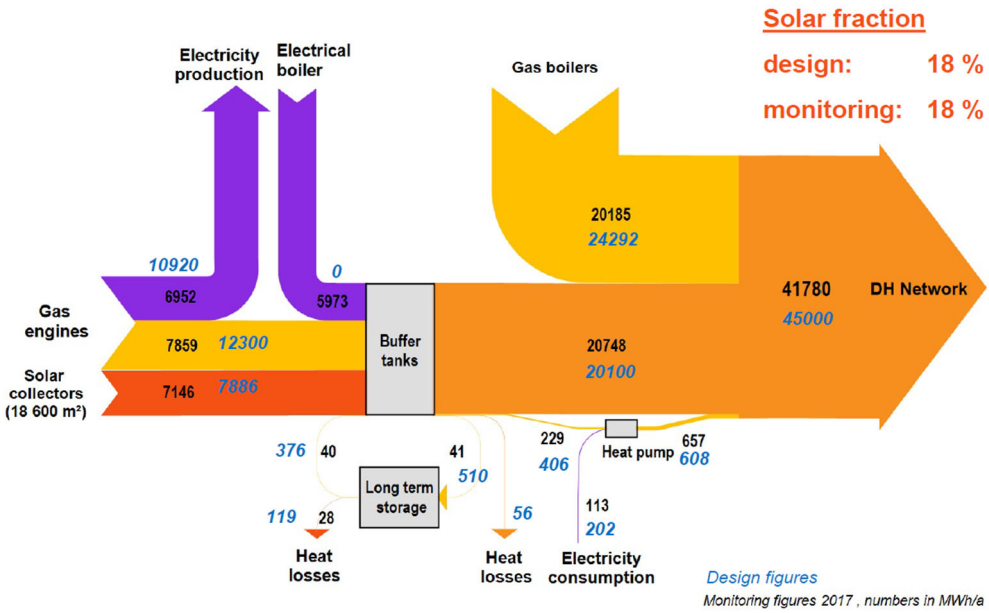

Figure 3.10. Energy flow diagram for the solar heating system in 2017 (blue figures represent the design figures).

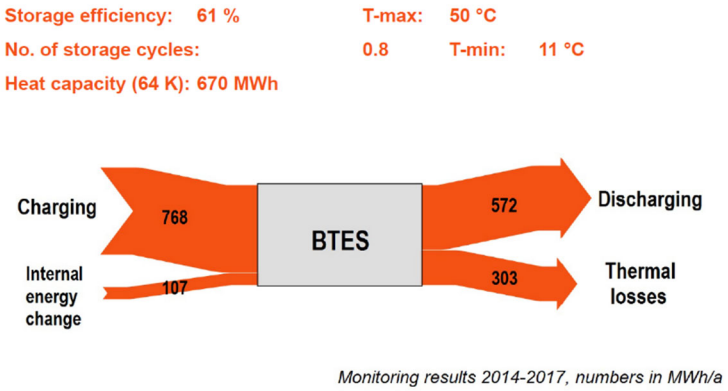

Figure 3.11. BTES energy flow diagram, years 2014 to 2017.

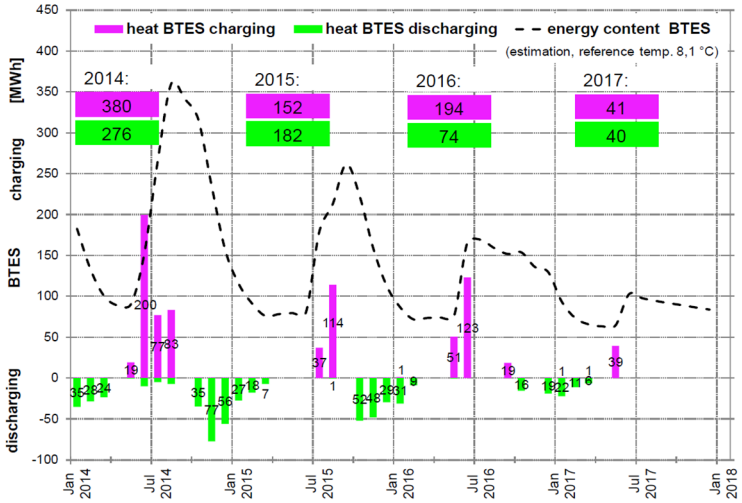

Figure 3.12. BTES energy balance evolution (charging and discharging) from 2014 to 2017.

3.1.2 BTES measurements description

A series of sensors have been installed in and around the BTES, in order to follow up on the behavior of the BTES. The measurements made by these sensors can also be used as a reference for the calibration of the TRNSYS BTES models. The following section presents the types and location of the sensors used specifically for the BTES.

3.1.2.1 Sensor types and placement

The BTES has been equipped with:

- A flow meter sensor placed on one of the inlet/outlet pipes of the BTES (measuring total flow from the building to the BTES)
- A temperature sensor on each one of the inlet/outlet pipes of the BTES
- Soil temperature sensors placed in 5 extra boreholes: 4 inside the boreholes area, and 1 outside (see Figure 3.14 for a cross section of the measurement boreholes and Figure 3.13 for the top view)
- Heat flux sensor placed on the top of the insulation (see Figure 3.13) plus 2 dedicated temperature sensors under and over the cover insulation on boreholes NDE 503 and 505 (see Figure 3.15)

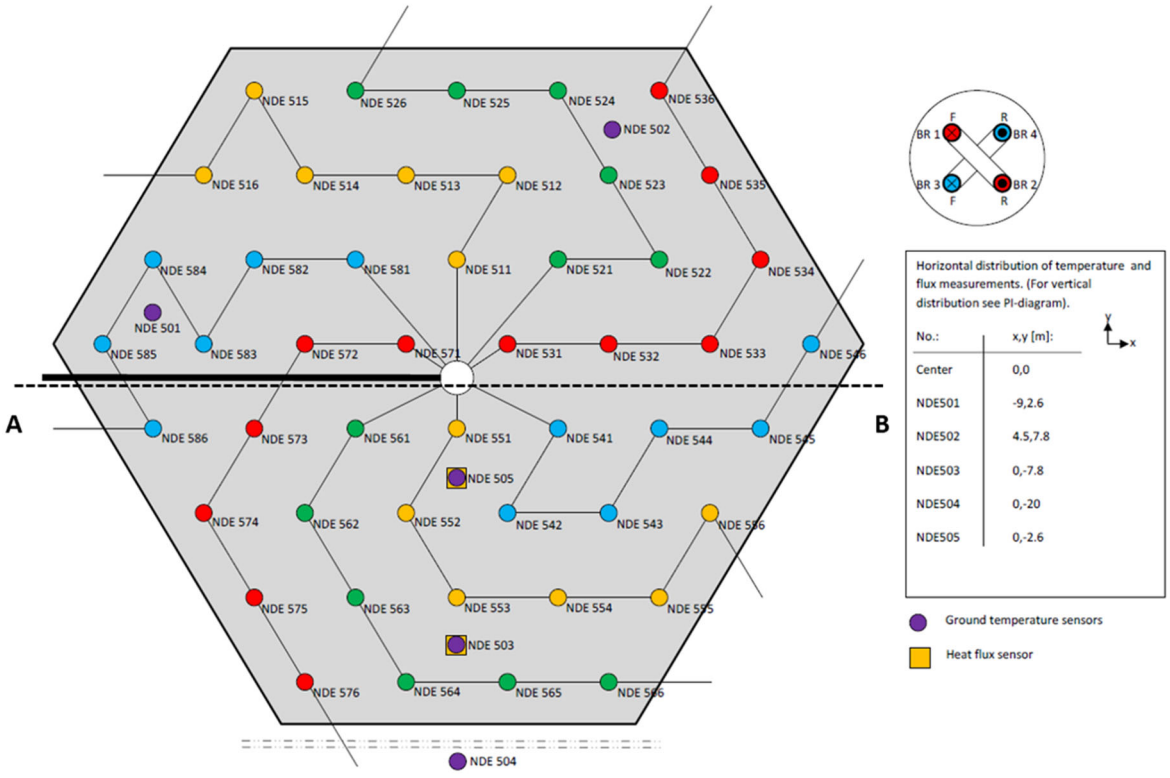

Figure 3.13. Top view of the BTES 48 boreholes and the extra 5 measurements boreholes, position of the given boreholes (box to the right) and top view of the double-U-pipes borehole heat exchangers implemented in each borehole (top right corner of the figure).

The temperature sensors have been placed in order to follow the evolution of soil temperature inside the BTES. They are therefore not distributed at equal distances/depths within each borehole (see Figure 3.15).

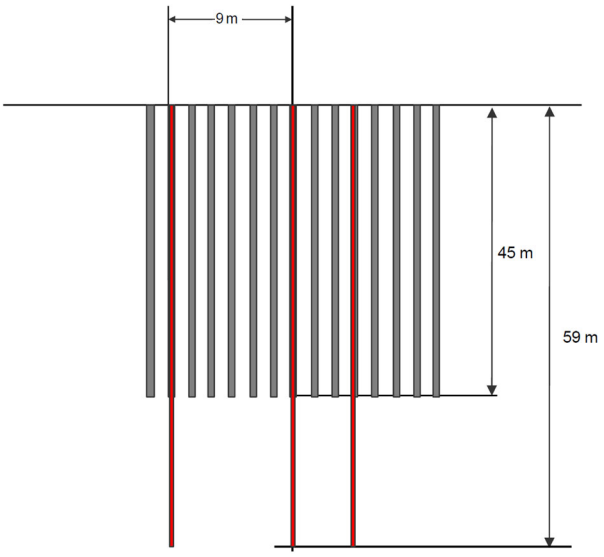

Figure 3.14. Cross section view (plan A-B from Figure 3.13) of the BTES boreholes including measurement boreholes.

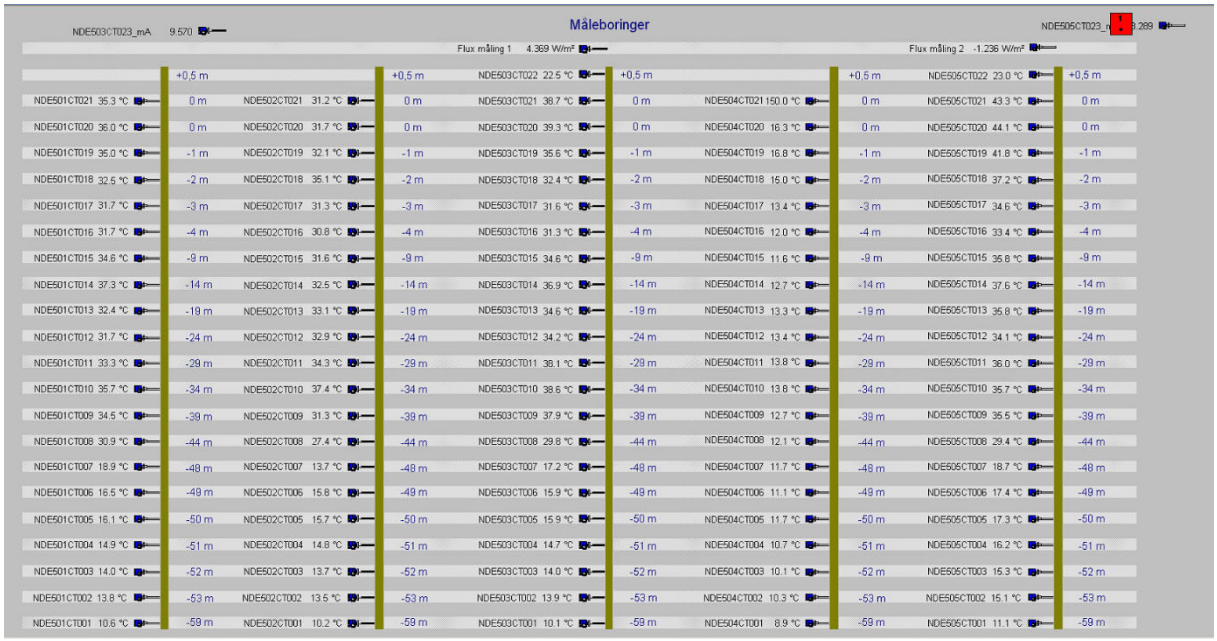

Figure 3.15. Screenshot of the monitoring user interface showing the temperature and flux sensors measurements for each measurement borehole.

3.1.2.2 Measurement campaign and method

The data recording system has constant time steps and the following time resolutions for the recording of data is used:

- For the borehole temperatures, a data point is recorded every 5 minutes
- For the flowrates and temperatures of the inlet/outlet pipes of the BTES, a data point is recorded every 5 minutes

These values are then averaged for every hour, and for temperatures associated with a flowrate, the mean values are weighted by flowrate:

$$T_{mean} = \frac{\sum_i T_i \dot{V}_i}{\sum_i \dot{V}_i}$$

For the calibration of the BTES model, data from the years 2014 and 2015 was chosen (see Section 3.1.1.5).

Based on the measurements of the temperature probes, and knowledge of the BTES volume, energy content can be calculated/estimated for every hour based on the BTES average measured temperature:

$$E_{content,BTES} = \rho_{soil} cp_{soil} V_{BTES} \left(\overline{T_{BTES}} - T_{ref}\right) = C_{soil}\, V_{BTES} \left(\overline{T_{BTES}} - T_{ref}\right)$$

where $E_{content,BTES}$ is the BTES energy content, calculated in MWh, ρ_{soil} is the soil density in kg/m^3, cp_{soil} is the soil heat capacity in J/kg/K, V_{BTES} is the BTES soil volume (19'200 m^3), $\overline{T_{BTES}}$ is the average BTES temperature, T_{ref} is the reference temperature, taken here as 8.1°C, and C_{soil} is the soil volumetric heat capacity in J/m^3/K.

All measurement boreholes inside the boreholes area (all boreholes except for NDE 504) are used to calculate the average temperature (see Figure 3.13).

After analyzing the temperature measurements results over the first years of operations, it was decided to use only the most relevant temperature sensors to evaluate $\overline{T_{BTES}}$, and they were estimated to be for each measurement borehole inside the boreholes area, temperature sensors 8 to 15 (between -9 m and -44 m, see Figure 3.15 and Figure 3.16).

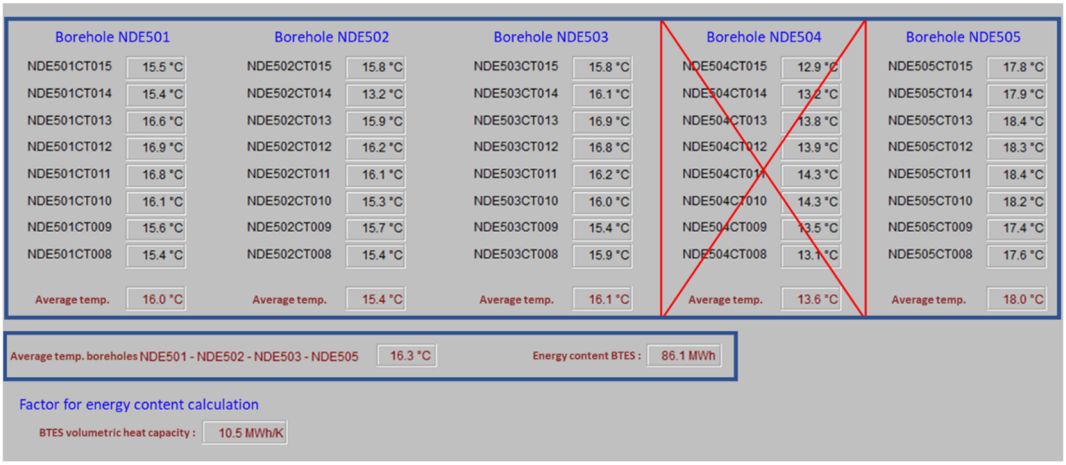

Figure 3.16. Temperature sensors used for the calculation of BTES energy content.

$\overline{T_{BTES}}$ is calculated as the average temperature of each measurement borehole (see Figure 3.16), for which the temperature is the average of temperature measurements provided by sensors 8 to 15:

$$\overline{T_{BTES}} = \frac{1}{4} \sum_{i\epsilon\{1,2,3,5\}} \overline{T_{NDE50i}}$$

with:

$$\overline{T_{NDE50i}} = \frac{1}{8} \sum_{j\epsilon[\![8,15]\!]} T_{NDE50iCTj}$$

and $T_{NDE50iCTj}$ is the hourly value of the temperature measured by sensor NDE50iCTj.

The global heat losses cannot be measured directly as there is no accessible and well-defined surface of the storage volume. They were therefore globally estimated by making a global annual energy balance (see Section 3.1.4.4).

Figure 3.17 shows some measurements from the pilot borehole storage from 2014 and 2015. The charged and discharged heat (accumulated energy) are calculated from the flow, the inlet and outlet temperatures.

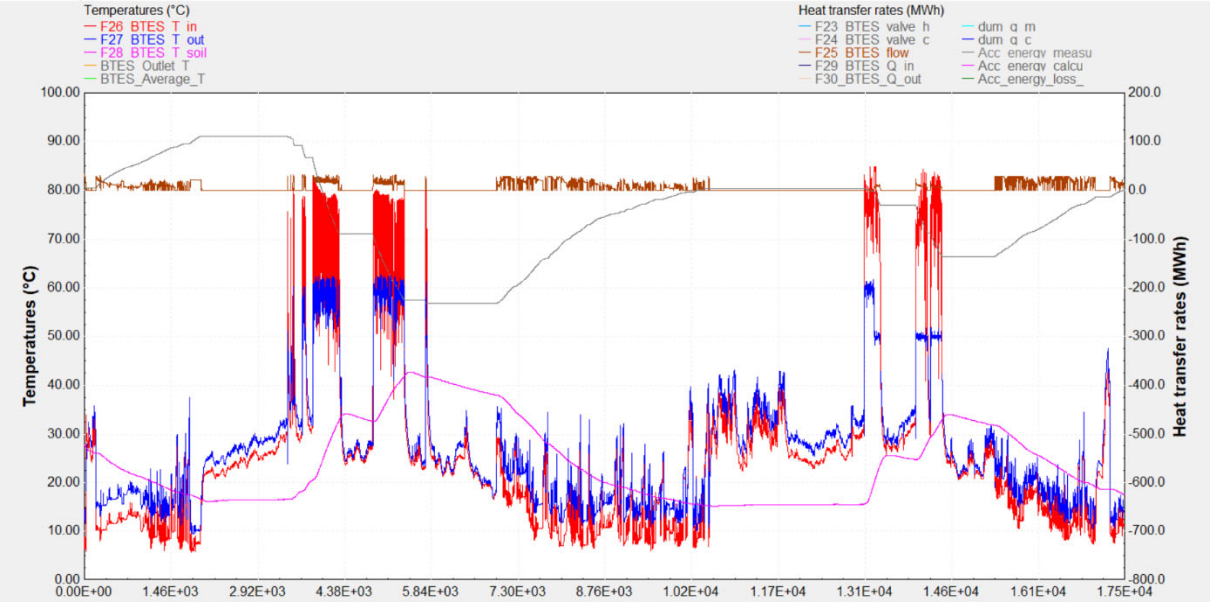

Figure 3.17. Measurements from the pilot borehole storage from 2014 and 2015. Left axis, red and blue = inlet and outlet temperatures, pink = average soil temperature in the storage [°C]. Right axis, brown = flow [m3/h], grey = calculated charging and discharging [MWh].

3.1.3 Modelling approach

When planning borehole thermal energy storage (BTES) projects, it is necessary to be able to accurately model the operation of the BTES within the energy system where it should be integrated in order to evaluate the feasibility of the project. Such modelling can be performed in the simulation environment TRNSYS, which has been used by PlanEnergi to model projects involving BTES for the past 10 years.

3.1.3.1 Presentation of the BTES component

TRNSYS offers one main component to model a BTES. It is called the Duct Ground Heat Storage Model ("DST" model for short, Type 557b in TRNSYS). This component models a BTES assuming that a given number of boreholes are placed uniformly within a cylindrical storage volume of soil. There is convective heat transfer within the pipes, and conductive heat transfer to the storage volume. The temperature in the ground is calculated from three parts; a global temperature, a local solution, and a steady-flux solution. The global and local problems are solved with the use of an explicit finite difference method. The steady flux solution is obtained analytically. The temperature is then calculated using superposition methods[12].

A principle diagram is shown in Figure 3.18. The numerical model uses the explicit finite difference method (FDM). The simulated ground volume is divided into a two-dimensional mesh using a radial coordinate r and a vertical coordinate z. A mesh is automatically generated and shows a more refined mesh at the edge of the boreholes area (top, sides and bottom, see right part of Figure 3.18). The model assumes homogeneous soil properties inside the boreholes volume, but outside, the soil can be divided into up to 10 layers of different thickness, thermal conductivity and volumetric heat capacity.

[12] Göran Hellström, Department of Mathematical Physics, University of Lund. "Duct Ground Heat Storage Model – Manual for Computer Code", March 1989.

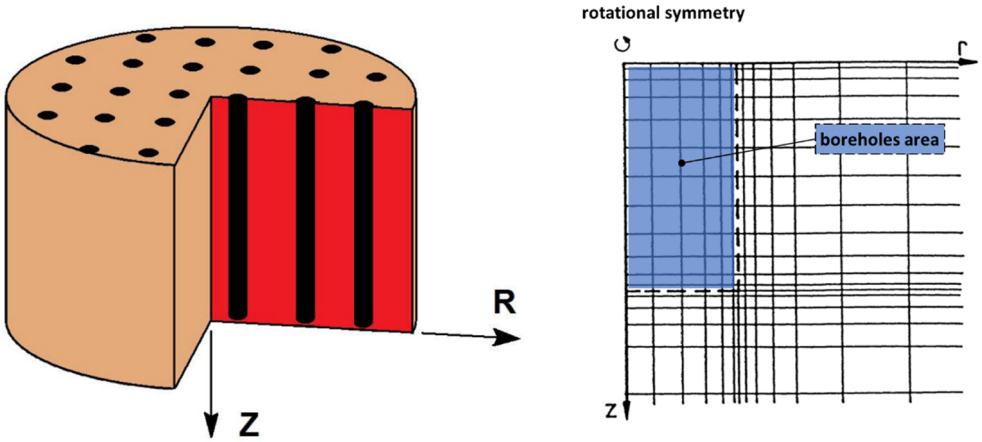

Figure 3.18. Geometry used to model the BTES in the DST TRNSYS model (left figure) and example of mesh (right figure, taken from the DST Manual for Computer Code[12]) used for the soil modelling in TRNSYS DST model.

3.1.3.2 Presentation of the calibration model and method

In this report, this TRNSYS BTES component is calibrated using measurement data from the BTES in Brædstrup in Denmark. The calibration is performed with data from the whole 2014 and 2015 years, in a resolution of 60 minutes. The measured input temperatures and flows etc. for the Brædstrup storage are given as input data to the BTES model, and the resulting calculated output temperatures, flows etc. from the simulation are then compared to the corresponding measured data in order to see which parameters reproduce best the conditions of the real BTES in Brædstrup.

The graphical layout of the TRNSYS model that was constructed for the calibration is shown in Figure 3.19. The model only consists of an input data file, giving flowrate, direction of the flow, and temperatures of the water at the inlet of the BTES (light green, thin lines). These inputs are gathered and then fed to the BTES component (light green, thick lines). No other components, such as heat exchangers, heat pumps, etc. are included in the model, because the aim of this model is to evaluate the performance of the BTES module only. The model also plots and prints the results (orange lines), calculates the error (the deviation in the model results from the measurement data, darker green lines) and summarizes the annual performance (by means of the integrator, brown lines). Parameters for the BTES are varied partly through the Control Cards (global constants in TRNSYS) and partly in the component “Param_BTES” (black dotted line).

For the BTES, only one version of BTES component is tested and calibrated (Type 557b).

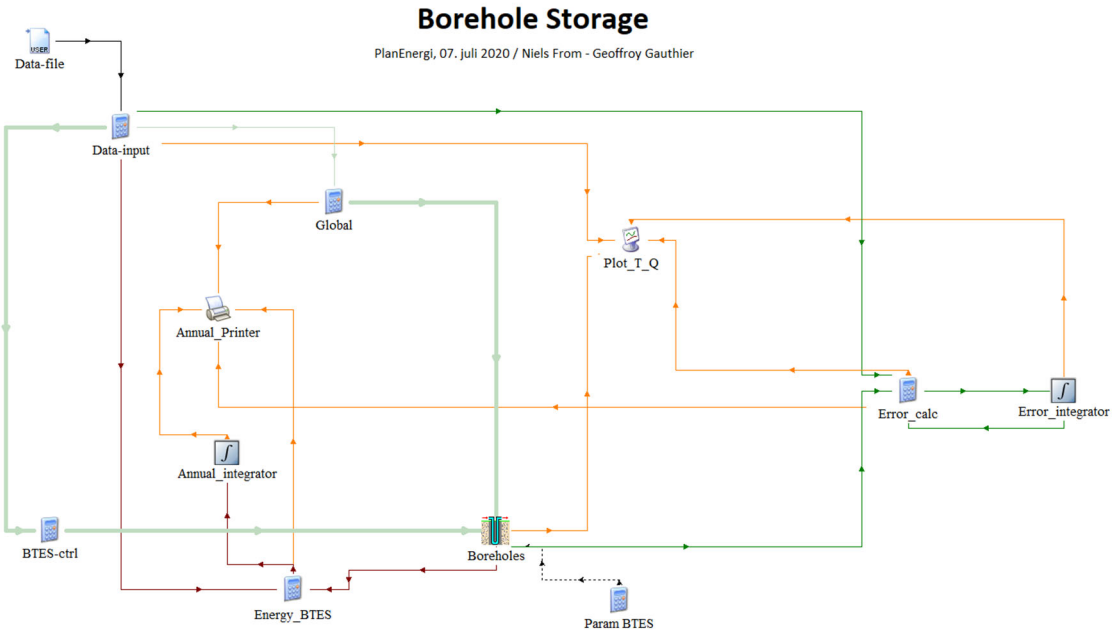

Figure 3.19. TRNSYS model layout used for the BTES calibration.

3.1.3.3 Calibration of the BTES component

Within Type 557b, parameters that are being calibrated in the present study can be segmented into 5 main categories:

1. Soil thermal properties inside the boreholes area (assumed homogeneous)
2. Soil thermal properties around the boreholes area (with possibility to divide this area into 10 layers with different thicknesses and thermal properties)
3. Insulation properties (thickness, thermal conductivity, extension over the soil around the boreholes area)
4. Grouting material properties (thermal properties of the boreholes' filling material)
5. Preheating conditions (parameters used to preheat the soil around the boreholes area)

Figure 3.20 illustrates the way the BTES soil was segmented for parametric optimization.

Type 577b allows the use of different thermal properties for the soil in the boreholes area and the soil in the area surrounding the boreholes area. Outside the boreholes area, the soil has been divided into 9 layers of 5 meters thickness to the side of the boreholes area, and one bottom layer of 45 m thickness under the boreholes area. This segmentation outside the boreholes area also allows for the use of different soil properties for each layer to the side of the BTES. However, in the present study, to simplify calibration, it was assumed that the top 9 layers have the same thermal properties, different from the thermal properties of the boreholes area and those of the bottom soil layer, outside of the boreholes area (see Figure 3.20).

These parameters are calibrated (varied) to obtain the best compliance between calculation and measurements (see Section 3.1.4 for calibration results). An optimization software, "GenOpt", was used to calibrate these parameters. GenOpt launches TRNSYS simulations and varies parameters in order to minimize a cost function.

GenOpt was used to find the value for a set of parameters (refer to Table 3.2) that maximizes the average of 3 coefficients of determination (see Section 2.1.4.1):

- one for the heat charged into the BTES
- one for the heat discharged from the BTES
- one for the average BTES temperature

This way, we calibrate the BTES component to model accurately the inlet and outlet heat flows through the BTES, as well as the average temperature of the BTES, which is proportional to the BTES energy content.

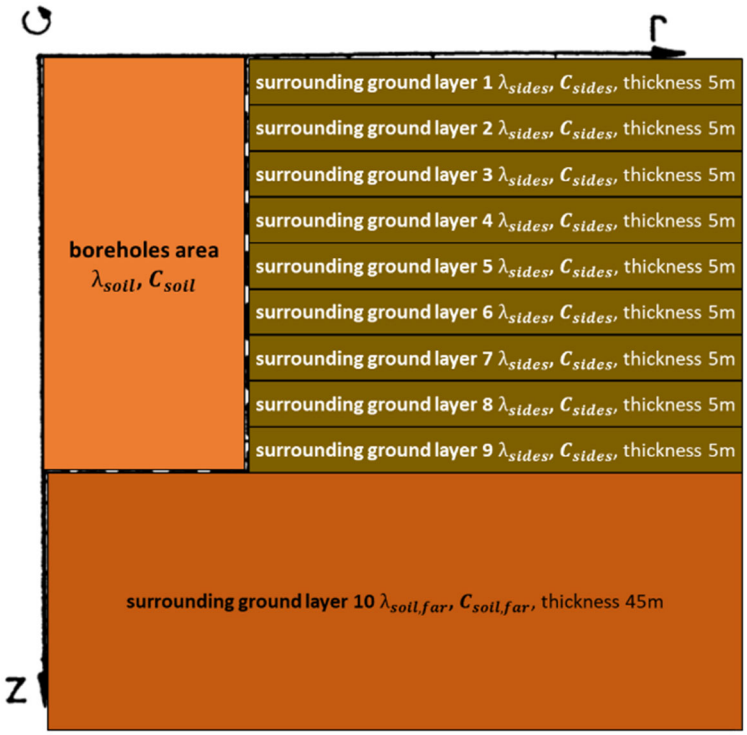

Figure 3.20. Representation of the BTES soil parameters' segmentation used for the calibration (not to scale). Insulation and grouting material (boreholes) aren't represented, for clarity.

Table 3.2. Main parameters used to set up the BTES model in TRNSYS.

Parameter	Unit	Initial value	Optimization
Storage Volume	m^3	19'200	Constant
Borehole depth	m	45	Constant
Header depth (depth of the top of the boreholes below the surface)	m	1	Constant
Number of boreholes	-	48	Constant
Borehole radius	m	0.075	Constant
Number of boreholes in series	-	6	Constant
Storage thermal conductivity	W/(m·K)	1.4	Calibrated
Storage volumetric heat capacity	J/(m^3K)	1'900	Calibrated
Fluid to ground resistance (borehole thermal resistance)[13]	m·K/W	0.172	Calibrated
Insulation thickness	m	0.5	Constant
Insulation thermal conductivity	W/(m·K)	0.12	Calibrated
Insulation extension over the boreholes area	m	3	Constant
Number of preheating years	-	2	Constant
Maximum preheat temperature	°C	45	Calibrated
Minimum preheat temperature	°C	10	Calibrated
Preheat phase delay	day	180	Calibrated
Average air temperature	°C	9.2	Constant
Amplitude of air temperature	°C	6.6	Constant
Air temperature phase delay	day	244	Constant
Number of ground layers (outside the boreholes area)	-	10	Constant
Thermal conductivity of layer i, $i \in [\![1;10]\!]$	W/(m·K)	1.4	Calibrated
Volumetric heat capacity of layer i, $i \in [\![1;10]\!]$	J/(m^3K)	1'900	Calibrated
Thickness of layer i, $i \in [\![1;10]\!]$	m	5 or 45[14]	Constant

[13] This parameter sets the global thermal resistance of every borehole (depends on the thermal properties of the grouting material, the boreholes' geometry, etc.).
[14] 5 m thickness for the first 9 layers, 45 m for the last layer, see Figure 3.20.

3.1.4 Calibration results

3.1.4.1 Methodology – Coefficient of determination

The same way a coefficient of calibration was calculated for various PTES parameters (see Section 2.1.4), coefficients of determination were calculated for the BTES heat input, heat output and average temperature. The calibration is based on maximizing the average of these coefficients, where mean coefficients of determination for heat input and output is averaged with coefficients of determination for mean temperature:

$$R^2_{global} = \frac{\frac{R^2_{BTES\_heat\_input} + R^2_{BTES\_heat\_output}}{2} + R^2_{BTES\_avg\_temperature}}{2}$$

3.1.4.2 Results presentation - calibration

The TRNSYS model using the non-calibrated parameters gives the simulation results presented in Figure 3.21. Calibrated parameters give the simulation results presented in Figure 3.22.

Table 3.3. Calibrated parameters resulting from the optimization calculations.

Parameter	Unit	Initial value	Calibrated value
Storage thermal conductivity	W/(m·K)	1.4	1.72
Storage volumetric heat capacity	J/(m³K)	1'900	1'900
Fluid to ground resistance (borehole thermal resistance)[15]	m·K/W	0.172	0.036
Insulation thermal conductivity	W/(m·K)	0.12	0.04
Maximum preheat temperature	°C	-	29
Minimum preheat temperature	°C	-	12
Preheat phase delay	day	-	68
Thermal conductivity of layer i, $i \in [\![1;9]\!]$	W/(m·K)	1.4	1.28
Volumetric heat capacity of layer i, $i \in [\![1;9]\!]$	J/(kg·K)	1'900	2'400
Thermal conductivity of layer 10	W/(m·K)	1.4	0.46
Volumetric heat capacity of layer 10	J/(m³K)	1'900	1'310

These parameters are in the range of the various thermal properties measured during the development phase for the pilot BTES in Brædstrup.

Figure 3.21 and Figure 3.23 show that without calibration (using design figures from Table 3.2, reusing only the preheat calibration parameters[16] from Table 3.3), the results of the calculations are much further off from the measurements.

Figure 3.22 shows that there is a good accordance between the measurements at the pilot borehole storage and the calibrated borehole storage model in TRNSYS, both for charged and discharged energy, as well as average BTES temperatures. This is confirmed by the coefficients of determination shown in Figure 3.23.

[15] This parameter sets the global thermal resistance of every borehole (depends on the thermal properties of the grouting material, the boreholes' geometry, etc.).
[16] The non-calibrated results reuse design parameters of the BTES, but since years 2014 to 2015 correspond the BTES operations after 2 years of charge-discharge, the preheating conditions obtained from the calibration were reused. They give more realistic start conditions for the soil temperatures and enable to see the influence of calibrating only the soil and insulation thermal properties.

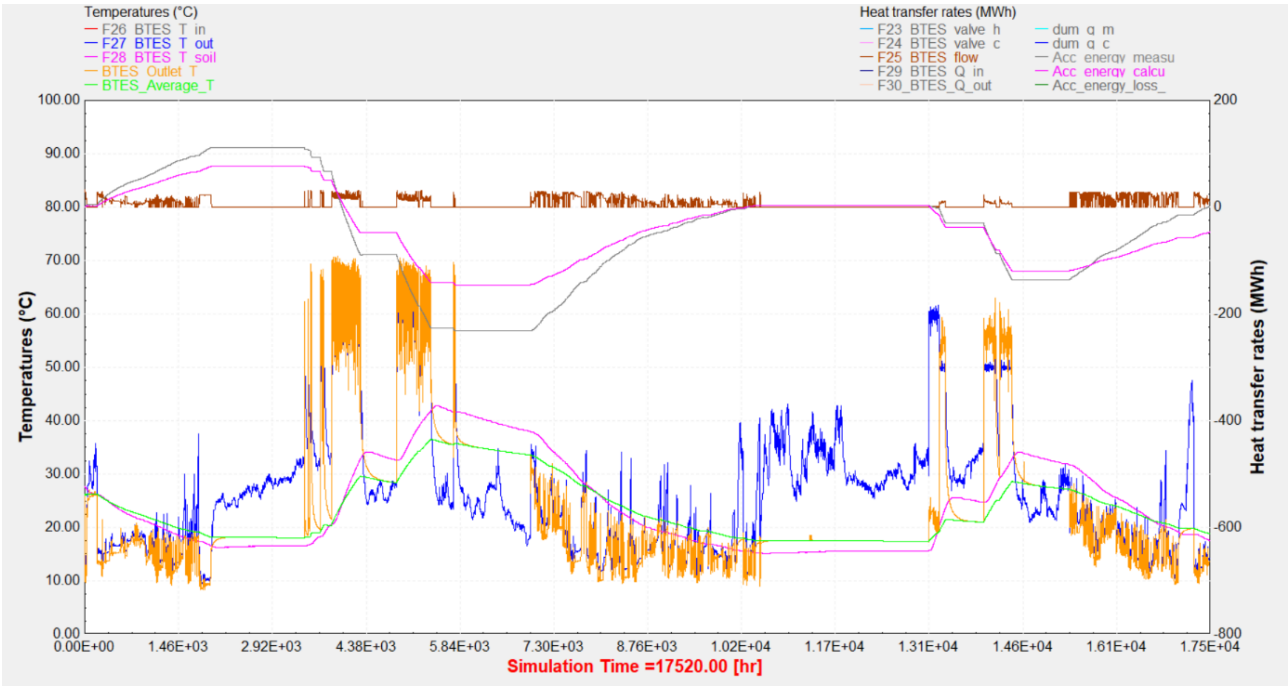

Figure 3.21. Comparison of measured and simulated values for 2014 and 2015, without calibration parameters. Left axis, blue = measured and orange = simulated outlet temperatures [°C], lower pink = measured and green = simulated storage temperatures [°C]. Right axis, brown = measured flow [m3/h], grey = measured and upper pink = simulated accumulated charged & discharged heat [MWh].

Figure 3.22. Comparison of measured and simulated values for 2014 and 2015, with calibration parameters. Left axis, blue = measured and orange = simulated outlet temperatures [°C], lower pink = measured and green = simulated storage temperatures [°C]. Right axis, brown = measured flow [m3/h], grey = measured and upper pink = simulated accumulated charged & discharged heat [MWh].

3.1.4.3 Results presentation – model prediction accuracy

Figure 3.23 shows the coefficients of determination for the calibrated BTES model as well as the not calibrated model. The global coefficient of determinations is determined by the formula from Section 3.1.4.1.

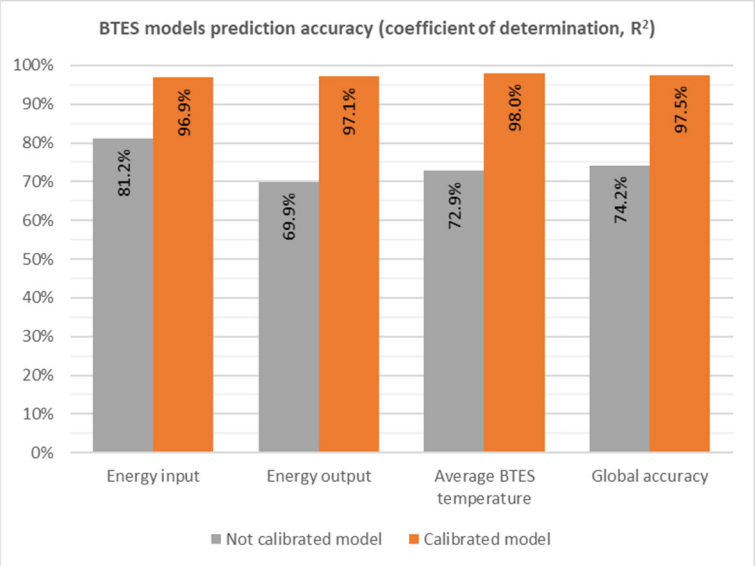

Figure 3.23. Model prediction accuracy for the calibrated BTES (in orange) and not calibrated BTES (in grey), shown in terms of the coefficient of determination (R^2), for average soil temperature, energy input & output, and global accuracy.

3.1.4.4 Results presentation – bi-annual energy balance

The other way to assess the model accuracy is by comparing annual energy balance for the BTES. Calculated energy input and output can be summed over the two calculated years 2014 and 2015, as well as heat losses through the lid, sides and bottom of the BTES. Calculation of energy content based on BTES average temperature also gives access to internal energy change for the BTES. These calculated values can be compared to measurements.

Since the heat losses for the BTES could not be calculated directly from measurements (not well-defined surface of the storage volume), they have been evaluated by making the following BTES heat balance:

$$BTES\ Internal\ Energy\ Change = Q_{BTES,in} - Q_{BTES,out} + Q_{BTES,losses}$$

where $Q_{BTES,in}$ and $Q_{BTES,out}$ are the sum of the heat respectively input into and taken from the BTES over 2014 and 2015, $Q_{BTES,losses}$ is the sum of the total heat losses through the top, sides and bottom of the BTES.

Results are presented in Figure 3.24 and show very good accordance between measurements and calculations from the calibrated BTES model.

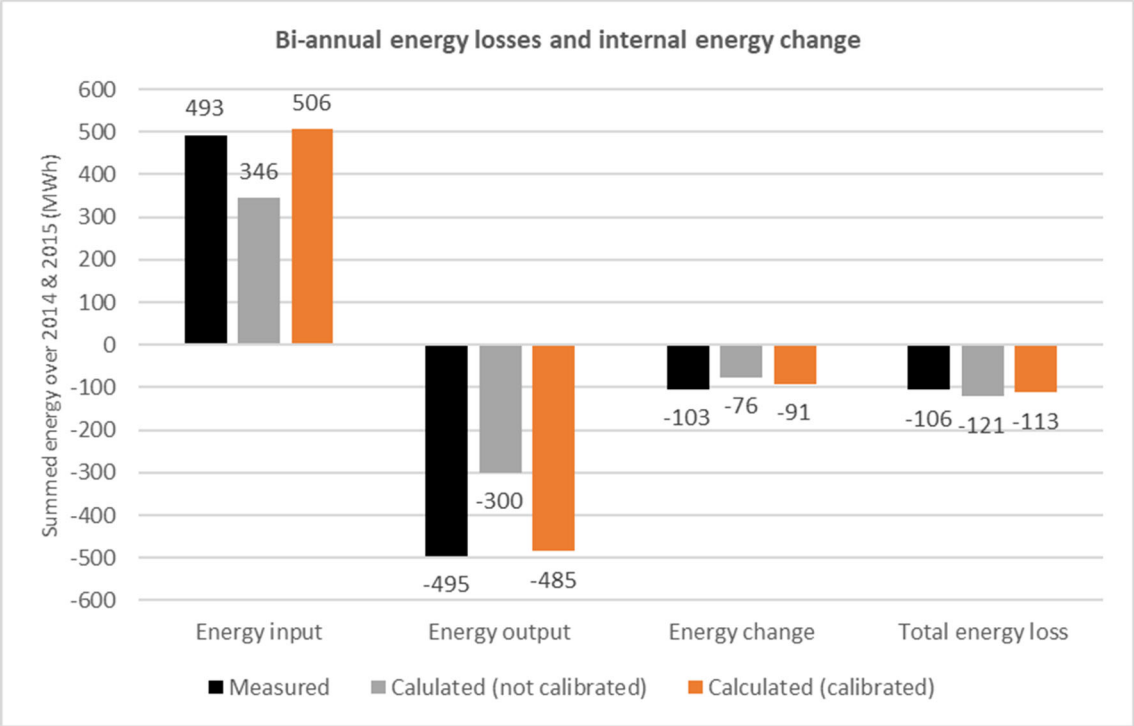

Figure 3.24. Bi-annual energy input, output, internal energy change and total energy losses of the BTES models. The black column shows the measurement data, to which the calibrated model results (in orange) and not calibrated model results (in grey) can be compared. All values are in MWh.

3.1.4.5 Results analysis

The results presented for the BTES model show the crucial importance of calibration for BTES modelling in TRNSYS. Without precise knowledge of soil and insulation material properties, it is impossible to predict accurately the heat balance for a BTES (see Figure 3.21 to Figure 3.24).

Once calibrated, it is possible to use calculations for energy balance predictions. The use of many temperature sensors is a great advantage and provides a reliable measurement reference. The difficulty for BTES model comparisons is the definition of the BTES volume, together with the BTES average temperature. In the present study, temperature sensors showing least important measurement variability were used to calculate average BTES temperature. This choice provides, after calibration, a good accordance between calculations and measurements, and energy balance over two years has been accurately modelled (see Figure 3.24).

When making feasibility studies for BTES projects, it is therefore highly recommended to get as many local soil properties as possible, to provide as parameters to the model:

- soil thermal response test
- soil samples inside the boreholes area
- soil samples outside the boreholes area, to the sides, and underneath
- precise borehole dimensions and grouting material properties